SHORT REPORT

Cytoskeleton
DOI10.1002/cm.21624

Acto-myosin dependent invasion of endothelial sprouts in collagen

Short title: Acto-myosin dependent invasion of sprouts

Marie-Mo Vaeyens[1] | Alvaro Jorge-Peñas[1] | Jorge Barrasa-Fano[1] | Apeksha Shapeti[1] | Maarten Roeffaers[2] | Hans Van Oosterwyck[1,3,@]

[1] Biomechanics Section (BMe), Department of Mechanical Engineering, KU Leuven, Leuven, Belgium;

[2] Centre for Membrane Separations, Adsorption, Catalysis and Spectroscopy for Sustainable Solutions (cMACS), Department of Microbial and Molecular Systems (M²S), KU Leuven, Leuven, Belgium;

[3] Prometheus, div. Skeletal Tissue Engineering, KU Leuven, Leuven, Belgium;

[@] Correspondence should be addressed to Hans Van Oosterwyck (Hans.VanOosterwyck@kuleuven.be).

ACKNOWLEDGMENTS

The authors are grateful for funding support from the Research Foundation Flanders (FWO) (FWO grants G.0821.13, G087018N, 1S68818N), from the Hercules-foundation (G0H6316N), from KU Leuven internal funding (C14/17/111) and from the European Research Council under the European Union's Seventh Framework Program (FP7/2007–2013)/ ERC Grant Agreement No. 308223) to H.V.O. We thank the Peter Carmeliet Lab for cell culture tips and techniques, Ben De Coninck for conducting 2D Traction Force Microscopy experiments and Leica Microsystems GmbH (Wetzlar, Germany) for access to and technical assistance with a Leica TCS SP8 STED microscope.

During sprouting angiogenesis – the growth of blood vessels from the existing vasculature - endothelial cells adopt an elongated invasive form and exert forces at cell-cell and cell-matrix interaction sites. These cell shape changes and cellular tractions require extensive reorganizations of the acto-myosin network. However, the respective roles of actin and myosin for endothelial sprouting are not fully elucidated. In this study, we further investigate these roles by treating 2D migrating and 3D sprouting endothelial cells with chemical compounds targeting either myosin or actin. These treatments affected the endothelial cytoskeleton drastically and reduced the invasive response in a compound-specific manner; pointing towards a tight control of the actin and myosin activity during sprouting. Clusters in the data further illustrate that endothelial sprout morphology is sensitive to the *in vitro* model mechanical micro-environment, and directs future research towards mechanical substrate guidance as a strategy for promoting engineered tissue vascularization. In summary, our

Cytoskeleton, doi: 10.1002/cm.21624

Received: Apr 16, 2020;Revised: Jun 11, 2020;Accepted: Jun 22, 2020

results add to a growing corpus of research highlighting a key role of the cytoskeleton for sprouting angiogenesis.

Key Words: *in vitro* angiogenesis, endothelial cytoskeleton, cellular force generation, blebbistatin, calyculin A, jasplakinolide, cytochalasin D

1 | Introduction

Angiogenesis, the formation of new blood vessels from the pre-existing vasculature (Betz, Lenard, Belting, & Affolter, 2016; Carmeliet, 2003; De Smet et al., 2009; Geudens & Gerhardt, 2011), occurs in physiological and pathological conditions and is a hallmark of a wide range of related diseases (Folkman, 2007). During sprouting angiogenesis, endothelial cells (EC) invade the extracellular matrix (ECM) by exerting cellular traction forces at cell-cell (Carmeliet, 2003; Huveneers et al., 2012) and cell-matrix (Edgar, Hoying, et al., 2014; Su, Mendoza, Kwak, & Bayless, 2008) interaction sites. Deciphering force generation by invading endothelial cells – a process that is highly dependent on the cytoskeletal architecture - is at the heart of understanding sprouting angiogenesis.

Endothelial cells have a mechanically tensed structure that preserves their shape (Goeckeler, Bridgman, & Wysolmerski, 2008; Ingber, 2008), while they can actively reorganize their cytoskeleton to remodel their shape and to generate traction forces (Carey, Charest, & Reinhart-King, 2010; Koestler, Auinger, Vinzenz, Rottner, & Small, 2008; Mseka & Cramer, 2011). To initiate sprouting from the quiescent vasculature, ECs convert from a flattened morphology to their elongated, invasive form (Hetheridge et al., 2012). ECs then migrate outwards as a collective entity of highly elongated cells, while follower cells are assumed to proliferate in a tension-dependent way (Haeger, Wolf, Zegers, & Friedl, 2015; Santos-Oliveira et al., 2015), parallel to the growth direction and thus facilitating the sprout elongation (Zeng et al., 2007). Within such a dynamic entity, traction forces generated by the leader cell are balanced by tensile forces at the cell-cell junctions of the follower cells at the rear (Friedl & Gilmour, 2009; Haeger et al., 2015). Follower cells may also contribute to the cellular traction forces by anchoring to the matrix with cryptic lamellipodia (Farooqui & Fenteany, 2005; Haeger et al., 2015). Tip cell extensions protrude in areas of local myosin depletion (which allows escaping cortical tension (Fischer, Gardel, Ma, Adelstein, & Waterman, 2009)) and probe the surrounding extracellular matrix for biochemical and mechanical cues. Actin-based cellular protrusions can guide 3D directional migration in response to mechano-chemical cues after adhering (Kubow, Conrad, & Horwitz, 2013; Thievessen et al., 2015) to a more distal and sufficiently stiff ECM for establishing acto-myosin contractility for movement in the new direction (Fischer et al., 2009). Acto-myosin contractility has been shown indispensable for sprout initiation (Kniazeva & Putnam, 2009), branching and orientation of invading endothelial cells (Elliott et al., 2015), capillary-like tube formation (Mabeta & Pepper, 2009), and sprout maintenance (Kniazeva & Putnam, 2009). However, limited data is available on quantifying tractions exerted by endothelial sprouts (Du et al., 2016; Du, Herath, Wang, Asada, & Chen, 2018; Kniazeva et al., 2012; Vaeyens et al., 2020; Yoon et al., 2019) and discrepancies exist between studies about the impact of cellular tractions on invasiveness (Indra et al., 2011; Koch, Münster, Bonakdar, Butler, & Fabry, 2012; Kraning-Rush, Califano, & Reinhart-King, 2012; Munevar, Wang, & Dembo, 2001; Peschetola et al., 2013). While tip cell pulling on stalk cells, stalk cell pushing on tip cells, or both, have previously been

postulated as mechanical forces that underlie sprout elongation (Betz et al., 2016; De Smet et al., 2009; Gerhardt, 2008; Geudens & Gerhardt, 2011; Santos-Oliveira et al., 2015; Sauteur et al., 2014; Schmidt et al., 2007; Travasso, 2011), collagen deformations indicative of tip cell pulling were recently reported (Vaeyens et al., 2020; Yoon et al., 2019).

Within the scope of this study, the respective roles of actin and myosin for sprouting angiogenesis were examined by targeting the acto-myosin network with chemical compounds (Figure 1). Blebbistatin and calyculin A were used to target non-muscle myosin II. Blebbistatin - a derivative of 1-phenyl-2-pyrrolidinone – selectively and potently blocks the myosin function by hindering a critical step of the ATPase cycle (Bond, Tumbarello, Kendrick-Jones, & Buss, 2013; Kovács, Tóth, Hetényi, Málnási-Csizmadia, & Seller, 2004), while calyculin A - isolated from marine sponge *Discodermia Calyx* - leads to an accumulation of hyperactivated myosins by inhibiting myosin dephosphorylation (Fabian, Troscianczuk, & Forer, 2007). A series of studies report decreased force generation of blebbistatin treated cells (Bondzie et al., 2016; Ghibaudo, Di Meglio, Hersen, & Ladoux, 2011; Jerrell & Parekh, 2014; Kraning-Rush, Carey, Califano, Smith, & Reinhart-King, 2011; Lemmon, Chen, & Romer, 2009), and increased cellular traction forces upon calyculin A treatment (Jerrell & Parekh, 2014; Lemmon et al., 2009; Stricker, Aratyn-Schaus, Oakes, & Gardel, 2011). Antagonistic effects for blebbistatin and calyculin A have also been demonstrated for cell-cell tugging forces (Liu et al., 2010) and cellular stiffness (Lu, Oswald, Ngu, & Yin, 2008): increasing contractility with calyculin A increased cell-cell tugging forces and cell stiffness, while decreasing contractility with blebbistatin decayed cell-cell tugging forces and lowered cell stiffness.

To target the actin component of the cytoskeleton, cytochalasin D and jasplakinolide were used. Cytochalasin D - a fungal metabolite extracted from *Metarrhizium anisopliae* – blocks actin filament elongation by binding the growing barbed ends of actin filaments (Scherlach, Boettger, Remme, & Hertweck, 2010; Wakatsuki, Schwab, Thompson, & Elson, 2001), while jasplakinolide (Bubb, Senderowicz, Sausville, Duncan, & Korn, 1994; Bubb, Spector, Beyer, & Fosen, 2000; Crews, Manes, & Boehler, 1986; Ju et al., 2010; Visegrády, Lorinczy, Hild, Somogyi, & Nyitrai, 2004) - a cyclic peptide extracted from marine sponge *Jaspis Johnstoni* – stabilizes actin filaments and potently induces actin polymerization by reducing the threshold for globular actin to bind to filamentous (F)-actin and by initiating nucleation cores *in vitro.* Cytochalasin D has been shown to decrease cellular tractions (Kraning-Rush et al., 2011), decrease cell-cell forces (Sim et al., 2015) and is being used as relaxation agent in 3D traction force microscopy experiments (Cóndor, Steinwachs, Mark, García-Aznar, & Fabry, 2017; Hall et al., 2013; Jorge-Peñas et al., 2017; Kim, Jones, Groves, & Sun, 2016; Koch et al., 2012; Malandrino, Trepat, Kamm, & Mak, 2019; Steinwachs et al., 2016; Vaeyens et al., 2020). While the literature seems overall consistent on the effect of blebbistatin, calyculin A and cytochalasin D on cellular tractions for a series of cell types, the published reports on the effect of jasplakinolide on cellular tractions appear less conclusive (Glazier et al., 2019; Goeckeler et al., 2008; Hui, Balagopalan, Samelson, & Upadhyaya, 2015; Hyland, Mertz, Forscher, & Dufresne, 2014; Jiang, Zhang, Yuan, & Poo, 2015). Therefore, it was experimentally validated how acto-myosin dependent cellular traction forces of endothelial cells are affected by jasplakinolide. Reduced tractions for jasplakinolide treated cells were expected from its mode of action, as the packing of actin at numerous nucleation cores leaves less actin monomers available for stress fiber turnover (Bubb et al., 2000).

The effect of the compounds on the endothelial cytoskeleton was first visualized in 2D EC cultures (Figure 1), showing characteristic rearrangements of the cytoskeleton and drastic shape changes. Next, we established an *in vitro* model of sprouting angiogenesis (Figure 2), and computational algorithms for quantifying invasion were developed (Figure 3). Finally the invasive responses of endothelial cells, treated with each of the compounds, were quantified (Figures 4-6). Clusters in the data further revealed that the endothelial cytoskeleton and sprout morphology are sensitive to the mechanical micro-environment of the *in vitro* setup. These observations are in agreement with the findings that cells sense and respond to micro-environmental mechanical and structural properties (Bordeleau et al., 2017; Charras & Sahai, 2014; Edgar, Underwood, Guilkey, Hoying, & Weiss, 2014; Fischer et al., 2009; P.-F. Lee, Bai, Smith, Bayless, & Yeh, 2013; Mason, Starchenko, Williams, Bonassar, & Reinhart-King, 2013; Miron-Mendoza, Seemann, & Grinnell, 2010; Myers, Applegate, Danuser, Fischer, & Waterman, 2011; Pedersen & Swartz, 2005; Shamloo & Heilshorn, 2010). Moreover, acto-myosin mediated contractility has been proposed to perform a critical mechanosensory role in translating changes in ECM mechanics and structure into altered cellular behaviour (Kniazeva & Putnam, 2009; Wolfenson et al., 2016). In this respect the sprout endothelial cytoskeleton not only has a physically supporting role, but also a regulatory one for guiding endothelial cell invasion and mediating branching dynamics. In brief, our results attribute a key role to the cytoskeleton for sprouting angiogenesis and direct future research towards mechanical substrate guidance as a strategy for promoting engineered tissue vascularization.

2 | Results and discussion

2.1 Targeting actin and myosin with chemical compounds

Endothelial cells treated with small molecules targeting actin and myosin as described above (and summarized in Figure 1b), exhibited characteristic effects on the F-actin cytoskeleton and cell shape compared to the control cells, as captured by confocal fluorescence microscopy. Concentrations were selected initially from literature and fixed at concentrations that still resulted in a confluent to near-confluent monolayer close to the interface with collagen after 24 hours of treatment. An overview of the chemical compounds with their binding target, mode of action and concentration used for the invasion experiments in this study is given in Supplementary Table 1. This table also provides references to published reports on viability assays with HUVECs for the used compounds for similar or higher concentrations (Conte et al., 2016; Iacobazzia et al., 2015; Kniazeva & Putnam, 2009; Sawyer, Norvell, Ponik, & Pavalko, 2001). At the concentrations used, compound-specific effects could be distinguished as visualized with brightfield microscopy at low magnification (Supplementary Figure S1). Blocking myosin activity with blebbistatin generated shriveled cells with reduced stress fiber density and abundant irregular membrane ruffles. Enhancing myosin activity with calyculin A also reduced stress fiber density but provoked well spread, compact, rounded cells (Figure 1a). Similar 2D shape changes in response to blebbistatin and calyculin A were reported previously for a series of cell types (Bloom, George, Celedon, Sun, & Wirtz, 2008; Bondzie et al., 2016; Kraning-Rush et al., 2011; Kubow et al., 2013). When targeting the actin polymerization, both blocking and promoting polymerization led to a heavily disrupted actin network, disappearance of stress fibers and overall cell shape changes (Figure 1a), as expected from literature (Braet, Spector, De Zanger,

& Wisse, 1998; Bubb et al., 2000; Conte et al., 2016; S. Lee et al., 2010; Mammoto, Mammoto, & Ingber, 2013; Nandakumar et al., 2004; Sasse, Kunze, Gronewold, & Reichenbach, 1998; Schliwa, 1982; Shoji, Ohashi, Sampei, Oikawa, & Mizuno, 2012; Silberberg et al., 2013; Waschke, Curry, Adamson, & Drenckhahn, 2004). Blocking polymerization with cytochalasin D resulted shortly after adding the compound in punctuate actin masses (not shown, as in (Kraning-Rush et al., 2011)), followed by an accumulation of actin at the cell periphery (Figure 1a). Increasing actin polymerization with jasplakinolide induced punctuate actin masses (similar as in (Braet et al., 1998)) followed by sites with actin excess in the perinuclear area (Figure 1a).

One of the greatest challenges when targeting the acto-myosin network from a chemical approach, lies in the (bio)specificity of the drugs used (Peterson & Mitchison, 2002), which is typically assessed by the affinity or binding energy, and the structural and chemical uniqueness of the binding site (Leckband & Israelachvili, 2001). While small molecules have proven their worth for *in vitro* studies, possible limitations of the compound-specificity should be considered alongside experimental results.

From the compounds used in this study, blebbistatin is known for its isoform specificity and its binding to myosin in an actin-detached state, this way preventing artefacts from the binding of non-functional acto-myosin complexes (Allingham, Smith, & Rayment, 2005; Bond et al., 2013; Kovács et al., 2004; Limouze, Straight, Mitchison, & Sellers, 2004; Straight et al., 2003). While calyculin A is known for its specificity for both PP1 and PP2A within the PPP family of phosphatases (as opposed to several other families of phosphatases) (Gupton & Waterman-Storer, 2006; Ishihara, Martin, et al., 1989; Ishihara, Ozaki, et al., 1989; Köhn, 2017), its mode of action also inhibits other members of this family (Swingle, Ni, & Honkanen, 2007) and a study from Holy et al. shows that calyculin A has at least dual pharmacological effects by affecting calcium levels next to phosphatase activity (Holy & Brautigan, 2012). Cytochalasin D shows actin specificity and has high affinity for capping barbed ends of actin filaments (Cooper, 1987), however, a more recent study shows that CytoD also affects the interaction between G-actin and G-actin-binding proteins (Shoji et al., 2012). The other actin-targeting compound used, jasplakinolide, binds F-actin with strong affinity (Bubb et al., 1994, 2000; Visegrády et al., 2004), and has been characterized as an actin-specific reagent that induces polymerization and stabilizes actin filaments (Holzinger, 2001). While recent structural conformation analysis by Pospich et al. shows that jasplakinolide traps actin in a natural state, their data also suggests jasplakinolide to interfere with the natural aging process of F-actin - which affects some of the actin-binding protein interactions - hereby disrupting the overall balance of the complex actin cytoskeletal system (Pospich, Merino, & Raunser, 2020).

Targeting the actin cytoskeleton and/or acto-myosin interaction, is further expected to have secondary effects through complex downstream signaling cascades (Hohmann & Dehghani, 2019), considering that the cytoskeleton plays a fundamental role in a wide range of cellular processes (Bogatcheva & Verin, 2008; Fletcher & Mullins, 2010; Hohmann & Dehghani, 2019), and because the actin cytoskeleton acts as a scaffold for many proteins. Because of this downstream signaling and also because of the close interaction of actin and myosin in contractile stress fibers, targeting actin can indirectly affect myosin function and vice versa (Goeckeler et al., 2008). In addition, actin and myosin are fundamental for force transmission from the extracellular environment via adhesional complexes down to the genetic material found in the nucleus (N. Wang, Tytell, & Ingber, 2009). The signaling cascades involved in mechanotransduction (Provenzano & Keely, 2011), display complex crosstalk with signaling cascades regulating angiogenesis

(Ingber, 2002; Katoh, Kano, & Ookawara, 2008). As a striking illustration of downstream effects when targeting actin, Wang et al. demonstrated how 4h of jasplakinolide treatment caused altered transcriptional regulation of 224 genes in HUVEC cells (Shuaijun Wang et al., 2019).

2.2 Visualizing the endothelial sprout cytoskeleton and semi-automated quantification of the invasive response

As *in vitro* model of angiogenesis, we adapted the model described by Bayless in 2009 (Bayless, Kwak, & Su, 2009; Vaeyens et al., 2020), which allows visualizing the cytoskeleton of sprouting human umbilical vein endothelial cells (HUVEC) at higher magnification (Figure 2 and Supplementary Figure S2). Figures 2b-e illustrate the actin cytoskeleton of sprouts and sprout tips within this model with increasing level of detail. As expected, the cytoskeletal organisation within EC sprouting into a 3D collagen differed markedly from the cytoskeleton of 2D spread cells, which typically displayed more pronounced stress fibers (Figure 1a, Ctr).

For quantifying the sprouting response, we established computational algorithms (see Methods) for filtering microscopy data (Figure 3a), identifying the hydrogel interface (with cell layer attached to hydrogel lateral surface, see Supplementary Figure S2a-c), determining the maximum invasion distance (Figure 3b), detecting the detached sprouts (Figure 3c), measuring the total projected sprout area (Figure 3d), and counting the nuclei within the field of view or within the segmented sprout area (Figure 3e,f). Microscopy data from the sprout samples was collected by z-scanning approximately 550 µm stacks with an inverted confocal fluorescence microscope (Supplementary Figure S2c). The upper and lower boundaries of the samples could be detected from distinct peaks in the fluorescence signal because of HUVEC cells spreading on the dish bottom (Supplementary Figure S2c, peak close to $z = 0$) and dish top cover (Supplementary Figure S2c, peak close to $z = 550$ µm).

Quantification of sprouts grown without pharmacological treatment revealed differences in the invasive response depending on the height within the z stack (see Supplementary Figure S3a-c and Supplementary Table 2), and which was subdivided into regions near the dish bottom (ROI I), in the central part of the gel (ROI II), and near the dish top cover (ROI III). Compared to sprouts in the other two regions, sprouts in ROI I were longer (Supplementary Figure S3d), more abundant (Supplementary Figure S3e), composed of a higher number of cells (Supplementary Figure S3f) and occasionally resembled the sheet-like invasion described by Vickerman *et al.* (Vickerman, Blundo, Chung, & Kamm, 2008; Vickerman, Kim, & Kamm, 2013). High magnification imaging revealed sprouts in vicinity of the rigid dish bottom that were forming in a 2D planar-like manner (more spread, pronounced stress fibers, Supplementary Figure S3g) resembling 2D spread planar cells (Supplementary Figure S3i), while in the bulk region of the gel sprouts were consistently forming in a 3D spindle-like manner (thinner, spikier, Supplementary Figure S3h), resembling typically spindle-like HUVECs embedded in collagen (Supplementary Figure S3j). Lastly, the differences in overall invasive response between ROI I and II (Supplementary Figure 3d-f) were also affected by myosin activity, with blebbistatin treatment slightly reducing this difference compared to control conditions (significantly smaller ratio ROI I/ROI II for sprout area in case of blebbistatin) and calyculin A treatment slightly increasing this difference (significantly larger ratios ROI I/ROI II for sprout distance, area and number of nuclei in case of calyculin A compared to blebbistatin) (Supplementary Figure 3k and Supplementary Table 2). As several studies put forward that dimensionality sensing is myosin dependent (Doyle, Wang, Matsumoto, & Yamada, 2009; Hung et al., 2013; Ng, Besser, Danuser, & Brugge, 2012;

Oakes, Banerjee, Marchetti, & Gardel, 2014; Winer, Oake, & Janmey, 2009), this suggests that the regional difference was at least partially linked to substrate dimensionality, as previously described (Cavo et al., 2016; Doyle, Petrie, Kutys, & Yamada, 2013; Fraley et al., 2010; Martins & Kolega, 2006). ROI III surprisingly lacked sprouts in many samples, and upon inspection of this region, the collagen in the chamber device in these cases had contracted slightly from the top and side of the dish – as reported before by Sung *et al.* (Sung et al., 2010), preventing consistent data collection near the dish cover. To account for the above results, the invasive response in this study was further quantified by imaging the full stack of the samples and the total z-projected data stacks were compared, comprising all regions for all samples. Unless specified differently, presented invasion data is based on the quantifications of the coherent sprouts (without the detached tip cells). For completeness, we note here that the trends of the averages of the invasion metrics for the different conditions were similar based on the data including the detached tip cells.

2.3 Myosin-dependent sprout progression and branching

To verify that endothelial cell sprouting into collagen in our *in vitro* model is myosin force dependent as previously reported for EC sprouts in fibrin (Kniazeva & Putnam, 2009; Kniazeva et al., 2012) and aortic explants from transgenic donor mice in collagen (Elliott et al., 2015), we grew sprouts while impairing myosin-dependent cellular tractions with the commonly used small molecule blebbistatin (Bloom et al., 2008; Bondzie et al., 2016; Ghibaudo et al., 2011; Gjorevski, Piotrowski, Varner, & Nelson, 2015; Kniazeva et al., 2012; Moreno-Arotzena, Borau, Movilla, Vicente-Manzanares, & Garcia-Aznar, 2015; Yoon et al., 2019), which sequesters myosin in the non-active state (Figure 4a). The effect on sprout cytoskeleton and morphology in our model is shown in Figure 4b-e. Blebbistatin treated sprouts typically displayed arboreal, branched protrusions compared to the control condition (Figure 4b). This can be caused by a lowered local cortical tension due to myosin depletion (Fischer et al., 2009; Tee, Fu, Chen, & Janmey, 2011) which allows protrusions to form (Fischer et al., 2009). The excessive amount of protrusions in response to blebbistatin may have led to the increased complexity of HUVEC cord formation found by Abraham *et al.* and the hypersprouting found by Wang *et al.* (Abraham et al., 2009; Shue Wang et al., 2017). Quantification of our data showed overall shorter sprouts (Figure 4d), with less sprout surface area (Figure 4c), but a similar number of invading cells (Figure 4e). Inhibiting myosin-dependent contractility thus blocked sprout progression rather than initiation. While we expected reduced cell-cell connectivity (Breslin, Zhang, Worthylake, & Souza-Smith, 2015; Chervin-Pétinot et al., 2012) and more detaching tip cells upon blebbistatin treatment (Yoon et al., 2019), quantifications of the ratio between sprout area and detached cell area did not show significant differences with the control condition. Detaching tip cells did migrate less far than the control (Supplementary Table 3), concordantly to the fact that reduced myosin activity in single cells has been shown to perturb front-back polarity of migrating cells (Kolega, 2006), to decrease 3D cell migration rates (Doyle, Carvajal, Jin, Matsumoto, & Yamada, 2015), to affect the nucleus shape (Versaevel, Grevesse, & Gabriele, 2012), to slow down the nucleus rotation (Kumar, Maitra, Sumit, Ramaswamy, & Shivashankar, 2014) and especially also to hinder the nuclear pushing in a 3D environment (Petrie, Koo, & Yamada, 2014).

Considering that sprouts myosin-dependently pull on their substrate to progress, an increased traction force potential could provide the cells with the means to more efficiently progress. Next, we thus investigated whether increasing the myosin-dependent cellular traction potential with calyculin A (Jerrell & Parekh, 2014; Kraning-Rush et al., 2011; Lemmon et al., 2009; Liu et al., 2010) would positively correlate with

invasion. However, calyculin A did not promote sprout progression, but on the contrary reduced the overall invasion and lead to highly disrupted sprout morphology. Quantification showed that a significantly smaller number of cells initiated invasion (Figure 5e). Sprouts were shorter (Figure 5d), showed a more compact morphology (Figure 5b) - similar to the more rounded cellular morphology in 2D migrating cells - and covered a smaller invasion area (Figure 5c). Sprouts did have (proportionally) less detaching sprout area, suggesting improved sprout integrity and thus tighter cell-cell interactions, as previously quantified for pulmonary artery EC by Liu *et al.* (Liu et al., 2010). Impaired sprouting of cells with an increased traction potential can be understood by considering an optimal traction potential for optimal adhesion; sufficiently to pull and move forward, but not too tight which would reduce dynamics. An increased traction potential might thus have caused the EC to adhere so strongly to their substrate, that cellular dynamics were reduced and sprouting impaired. Interestingly, a study from Mierke demonstrates how calyculin A treatment could increase invasion of cells with lowered integrin expression, but not invasion of cells with wild type integrin levels (Mierke, 2013). In addition, sprouts also extend filopodia for probing and guiding the sprout through the matrix (De Smet et al., 2009) and for these filopodia to form, cortical tension needs to be lowered by local myosin depletion (Fischer et al., 2009). Finally, sprouting cells require elongation (Sauteur et al., 2014), while increasing the traction potential with calyculin A promotes the cells to contract into more compact, rounded cells (Figure 1). Increasing tractions at higher concentrations has even shown to completely round up cells and cause detachment from the substrate (Chartier et al., 1991). Taken together, we conclude that although cellular tractions are required for endothelial invasion into collagen, increasing cellular traction potential with calyculin A does not suffice to increase the invasive response.

2.4 Actin-dependent sprout progression and traction forces

Finally, we targeted forces originating from actin polymerization - which have been proposed to play a pushing role in sprout elongation (Sauteur et al., 2014) - by reducing or inducing actin polymerization with cytochalasin D and jasplakinolide respectively - as sketched in Figure 6a.

In sprouts with perturbed actin dynamics, accumulation of F-actin could be found, either at cell-cell boundaries within CytoD treated sprouts or perinuclear within Jasp treated sprouts, similar to the ones observed in treated spread cells (Figure 1 and Figure 6b). Disrupting the actin balance with either one small molecule hindered overall sprout invasion; leading on average to significantly less sprout area (Figure 6c), a shorter invasion distance (Figure 6d), and less invading cells initiating the sprouting (Figure 6e) compared to the control cells of the corresponding days treated with DMSO (see significance levels in Supplementary Table 3). The effect was more dramatically when blocking polymerization with CytoD than by inducing an excess with Jasp.

While blocking polymerization with cytochalasin D could directly interfere with filopodia formation – for which actin is found essential (De Smet et al., 2009), it is less straightforward how increasing polymerization with jasplakinolide could slow down sprout progression. From the mode of action of jasplakinolide, it has been proposed that sequestering the actin in non-functional masses, impairs the turnover and functionality of the stress fibers (Bubb et al., 2000). We therefore hypothesized that targeting the actin network also affected the sprouting through altered cellular traction forces. Because of inconsistencies in literature regarding the effect of jasplakinolide on cellular forces (Glazier et al., 2019; Goeckeler et al., 2008; Hui et al., 2015; Hyland et al., 2014; Jiang et al., 2015), Traction Force Microscopy

experiments were conducted to verify that acto-myosin dependent cellular traction forces of endothelial cells are indeed affected by jasplakinolide. Traction Force Microscopy experiments on PA gels coated with collagen showed that both increasing and reducing actin polymerization resulted in significantly lower total forces (Figure 6d, Supplementary Figure S4 and Supplementary Table 4). These results suggest that an imbalance of available actin reduces sprouting not only through reduced polymerization forces pushing at the membrane for filopodia formation and sprout elongation, but also by impairing the acto-myosin dependent cellular forces required to pull the sprout forward.

In contrast to our results, Jasp has been found to promote HUVEC adhesion, migration and tube formation by Jing *et al.* (Jing et al., 2013). Possibly this is due to differences in experimental model, as the experiments by Jing *et al.* were performed with 2D assays. This indicates once again crosstalk between acto-myosin contractility and the matrix mechanical micro-environment.

In summary, we investigated the respective roles of actin and myosin for sprouting angiogenesis by targeting endothelial cells with chemical compounds within an *in vitro* model of angiogenesis that allows visualization of the cytoskeleton at higher magnification. Analyzing the invasive response of cells under treatment of actin or myosin targeting compounds - as summarized in Supplementary Figure S5 - confirmed previously published reports that endothelial invasion is acto-myosin dependent (Elliott et al., 2015; Kniazeva & Putnam, 2009; Mabeta & Pepper, 2009), as invasion was significantly reduced by all compounds, in a compound-specific manner. Blebbistatin reduced sprout progression and induced more branching, while calyculin A halted both sprout initiation and progression, and showed less detaching tip cells. Cytochalasin D and jasplakinolide reduced sprout progression, at least partially through reduced cellular traction forces. The invasion response of untreated cells revealed positional effects within the model, that could be linked to substrate dimensionality. As this complements preceding research that mechanical stimulation has been shown to improve engineered vascularized grafts (Ceccarelli, Cheng, & Putnam, 2012), we direct future research towards matrix mechanics as an engineering approach of special interest for promoting engineered tissue vascularization. These results contribute towards a more fundamental understanding of the interdependence of sprouting angiogenesis, endothelial cytoskeleton mediated cellular traction forces and reciprocal sprout-matrix interactions.

Materials and Methods

HUVEC cell culture and fluorescence protocols

Pooled wild type human umbilical vein endothelial cells (HUVEC) were purchased at passage 1 (HUVEC, Angio-Proteomie, Boston, US, #cAP-0001), subcultured at approximately 90% confluency and used for invasion experiments up to passage 6. The cells were maintained in complete endothelial growth medium (EGM™-2 BulletKit™, Lonza, Basel, Switzerland, #CC-3162), which was exchanged 3 times per week. Approximately 70 % confluent wild type HUVEC cells were transduced with adenoviral LifeAct-GFP2 or LifeAct-RFP (Ibidi, Gräfelfing, Germany, #60121) at a multiplicity of infection (MOI) of 10 and incubated for 16 to 24h. Alternatively, wild type samples were fixed after 24h of sprouting with 4% methanol-free formaldehyde, stained with phalloidin (Alexa488-phalloidin, Invitrogen, Waltham, US, #A12379) overnight and with DAPI (Invitrogen, #D1306) for 30 minutes the following day.

Rat tail collagen type I hydrogel preparation

Collagen mixtures with a total volume of 1 ml before casting hydrogels were prepared on ice in a 50 ml conical tube by mixing collagen type I (Merck Millipore, Burlington, US, #08-115) with 150 µl sodium bicarbonate buffer (15.6 mg/ml), 5 µl of fluorescent bead solution (2% solids, 0.2 µm diameter, carboxylated, ex/em 580/605, Invitrogen, Belgium) to allow visualisation of the hydrogel and the appropriate variable amount of EGM2 to a final collagen concentration of 1.5 mg/ml. To initiate the polymerization reaction, a pH switch of the acidic collagen mixture was induced by using 1 M sodium hydroxide, after which the collagen was supplemented with pro-angiogenic factor Sphingosine-1-Phosphate (S1P, Sigma-Aldrich, St. Louis, US, #49840) to a final concentration of 1 µM. An amount of 25 µl of the mixture was pipetted in an imaging chamber (Secure-Seal™ hybridization sealing systems, ThermoFisher Scientific, Waltham, US, #S-24732), which was pre-mounted in a culture dish (multiwell plate or petridish). The hydrogels were allowed to polymerize and equilibrate in an incubator with 5% CO_2 at 37°C for a minimum of 30 minutes, before proceeding with the cell seeding.

***In vitro* angiogenesis model**

The *in vitro* angiogenesis model (Fig. 2 and Supplementary Fig. S2) was an endothelial sprouting assay (Bayless et al., 2009), adapted for improved diffusion (Vaeyens et. al, 2020). In brief, imaging chambers with increased inlet opening for optimal diffusion of the chemical compounds were fixed to a culture dish and 25 µl of collagen was pipetted into one inlet and polymerized as described above. After polymerization, 50000 cells from a 70-90 % confluent HUVEC culture in 25 µl of EGM2 were seeded through the other inlet and the dish was incubated vertically for one hour at 37 °C, 5 % CO_2, allowing the cells to sink by gravity and to form a cell layer on the lateral side of the collagen. After one hour, the dish was placed back horizontally, and abundant medium was added to the sample. The cells were then allowed to either initiate sprouting before live imaging or sprout for 24h before fixing and staining.

Chemical compounds

Blebbistatin, cytochalasin D and jasplakinolide were purchased from Merck Millipore (Burlington, US, #203390, #250255 and #420107). Calyculin A was obtained from Sigma-Aldrich (St. Louis, US, #C5552-10UG). Compounds were added after one hour of cell settling on the collagen, and maintained in the medium for the duration of the 24 hours sprouting experiment. Compounds were applied to the sprouting cells at the following concentrations: 50 µM blebbistatin, 1 nM calyculin A, 50 nM cytochalasin D or 50

nM jasplakinolide. Test conditions were compared to the control condition from the corresponding day (cells treated with DMSO, Sigma-Aldrich, St. Louis, US, #D12345). Traction force experiments were conducted with 50 nM jasplakinolide and 500 nM cytochalasin D.

Microscopy imaging of sprouts

All invasion experiments were imaged with an inverted confocal laser scanning microscope (Olympus FluoView™FV1000-IX81, Olympus, Japan) with motorized focusing, environmental T and CO_2 control and a 20x/NA 0.4 CORR long working distance objective. For F-actin visualizations, several objectives were used: a Leica HC FL FLUOTAR 40x/NA 0.6 CORR long working distance objective, a Leica 60x/NA 0.8 water objective and a Leica 63x/NA 1.3 glycerol immersion objective for stimulated emission depletion microscopy (STED) on a Leica TCS SP8 STED microscope. For exciting the fluorophores from Phalloidin-488 (Excitation $_{max}$ / Emission $_{max}$ = 495/518 nm), LifeAct-GFP2 (483 / 506 nm) and LifeAct-RFP (555 / 584 nm), the cells were excited with a 488 laser for GFP2 or a 559 nm laser for RFP. For nuclei imaging, DAPI (Excitation $_{max}$ / Emission $_{max}$ = 358 /461 nm) was excited with a 405 laser. For high throughout imaging of the fixed sprouts, z-stacks of 600 planes * 512 pixels * 512 pixels were taken, with a z resolution of 0.2 pixels/µm and xy resolutions of 0.4 pixels/µm. For high quality imaging of selected sprouts to visualize the cytoskeleton, images were acquired with xyz resolutions up to 3 pixels/µm.

Traction force microscopy

Polyacrylamide (PA) gels with a stiffness of 1.4 kPa were prepared as before and as described in (Izquierdo-Álvarez et al., 2019; Tse & Engler, 2010). Carboxylate-modified red fluorescent microspheres (FluoSpheres®, ThermoFisher Scientific, Waltham, US, #F-8810) of 200 nm were used as fiducial markers at a 1:60 ratio. Gels were activated with sulpho-SANPAH (ThermoFisher Scientific, Waltham, US, #22589) and functionalized with 100 µg/ml of rat tail collagen I (Corning, Corning, US, #354249). Live imaging of the samples was performed using the Olympus Confocal Laser Scanning Microscope described above and the Leica HC FL FLUOTAR 40x/NA 0.6 CORR long working distance objective. A 488 nm laser was used for the excitation of cells tagged with LifeAct-GFP2, and a 559 nm laser for the beads. Stressed state images of the cell and beads were taken before and after treatment with acto-myosin force modifiers. Stable relaxed state images were taken after cell removal using SDS. An in-house software in MATLAB was used to calculate the movement of the fluorescent beads in the stressed images relative to the relaxed ones based on the cell segmentation. Displacements to retrieve tractions were calculated as previously studied using free form deformation (FFD), Tikhonov regularization, and Fourier transform traction cytometry (FTTC) (Jorge-Peñas et al., 2015).

Data processing & image analysis

In this work, in house image processing tools were developed in MATLAB for data analysis. For processing of the microscopy data, first images were denoised by means of median filtering. Next, a smoothing filter followed by a logarithmic transformation and a grey value stretching were applied to increase the image contrast. Nuclei images were additionally filtered with a difference of Gaussian (DoG) algorithm for enhancement of the nuclei structures. Finally, a z-projection of the image stack was computed. For image analysis, the segmentation of the sprouts, the detached cells and the nuclei was done as described next: A binarization of the cell and nuclei images was done based on Otsu's thresholding. Typically, two groups result from the binarization of the cell images: detached cells (binary components of small size) and sprouts connected to the endothelial cell layer (a binary component of large size). After identifying the largest binary component in the image, two binary masks were obtained: a binary mask D was defined setting to 1 the voxels corresponding to the detached cells and a second binary mask C was defined setting to 1 the pixels corresponding to the sprouts connected to the endothelial cell layer. The segmentation of the matrix was done in three steps: first, a binary image was generated by setting to 1 the pixels corresponding to the

background. Second, morphological closing was used to fill the holes inside the background. Finally, the convex hull of the resultant binary image was computed obtaining a matrix mask M. The intersection between the binarized nuclei images and mask M was used to keep only the nuclei belonging to the invading sprouts. The number of nuclei is given by the resultant binary connected components.

Additionally, the following metrics were defined:

- $distance = \max(res \cdot \mathrm{DT}(M) \cdot A)$

where res is the pixel size in µm, DT is the distance transform and mask A can refer to the sprouts connected to the endothelial cell layer mask C or the detached cells mask D.

- $area = res^2 \cdot \sum_{x=1}^{L} G_A(x)$

where L is the number of pixels in the image and $G_A = M \cap A$.

Statistics

The characterization experiments of untreated cells were repeated three independent times, with sprouts growing in a total of 13 gels, which were measured at three positions, resulting in 39 data stacks. Hypothesis tests were one-way nested ANOVA tests to take into account the day-dependent variability in the invasive response. The invasion experiments under pharmacological treatment were repeated three independent times to assess the variation per condition, with each time three replicates per condition and three positions imaged within each replicate, resulting in 27 data stacks per condition. Hypothesis tests were one-way nested ANOVA tests to take into account the day-dependent variability in the invasive response. The traction force experiments were repeated five to six independent times with six to seven cells per gel, giving a total number of cells per condition as indicated in Supplementary Figure S3. Hypothesis tests were one-way ANOVA tests based on the day averages.

Normality of data and model residuals was inspected with Shapiro-Wilk tests and rejected below the p = 0.01 significance level. While data arrays and model residuals from the characterization experiments and traction force microscopy experiments were normally distributed, the data from the invasion experiments under treatment showed some deviations from normality. For consistency of the data analysis, all features for all chemical conditions were assessed with the same nested ANOVA test model, by accepting the deviations of normality for the CytoD condition (see individual datapoints and boxplots in Figures 6c-e) and the detached cell area feature in all conditions.

All statistical computations were performed with MATLAB. In the figures, significant p-values of hypothesis tests are indicated by * for $p < 0.05$, ** for $p < 0.01$ and *** for $p < 0.001$.

Data availability

The data and code that support the findings of this study are available within the Supplementary Figures, Supplementary Tables, cited references or from the corresponding author upon reasonable request. Laboratory protocols are available on the website of the corresponding author: https://www.mech.kuleuven.be/en/bme/research/mechbio, by navigating to the Software and Protocols section.

References

Abraham, S., Yeo, M., Montero-Balaguer, M., Paterson, H., Dejana, E., Marshall, C. J., & Mavria, G. (2009). VE-cadherin-mediated cell-cell interaction suppresses sprouting via signaling to MLC2 phosphorylation. *Current Biology*, *19*:668–674. https://doi.org/10.1016/j.cub.2009.02.057

Allingham, J. S., Smith, R., & Rayment, I. (2005). The structural basis of blebbistatin inhibition and specificity for myosin II. *Nature Structural & Molecular Biology*, *12*:378–379. https://doi.org/10.1038/nsmb908

Bayless, K. J., Kwak, H.-I., & Su, S.-C. (2009). Investigating endothelial invasion and sprouting behavior in three-dimensional collagen matrices. *Nature Protocols*, *4*:1888–1898. https://doi.org/10.1038/nprot.2009.221

Betz, C., Lenard, A., Belting, H.-G., & Affolter, M. (2016). Cell behaviors and dynamics during angiogenesis. *Development*, *143*:2249–2260. https://doi.org/10.1242/dev.135616

Bloom, R. J., George, J. P., Celedon, A., Sun, S. X., & Wirtz, D. (2008). Mapping local matrix remodeling induced by a migrating tumor cell using three-Dimensional Multiple-Particle Tracking. *Biophysical Journal*, *95*:4077–4088. https://doi.org/10.1529/biophysj.108.132738

Bogatcheva, N. V., & Verin, A. D. (2008). The role of cytoskeleton in the regulation of vascular endothelial barrier function. *Microvascular Research*, *76*:202–207. https://doi.org/10.1016/j.mvr.2008.06.003

Bond, L. M., Tumbarello, D. A., Kendrick-Jones, J., & Buss, F. (2013). Small-molecule inhibitors of myosin proteins. *Future Medicinal Chemistry*, *5*:41–52. https://doi.org/10.4155/fmc.12.185

Bondzie, P. A., Chen, H. A., Cao, M. Z., Tomolonis, J. A., He, F., Pollak, M. R., & Henderson, J. M. (2016). Non-muscle myosin-IIA is critical for podocyte f-actin organization, contractility, and attenuation of cell motility. *Cytoskeleton*, *73*:377–395. https://doi.org/10.1002/cm.21313

Bordeleau, F., Mason, B. N., Lollis, E. M., Mazzola, M., Zanotelli, M. R., Somasegar, S., … Reinhart-King, C. A. (2017). Matrix stiffening promotes a tumor vasculature phenotype. *Proceedings of the National Academy of Sciences of the United States of America*, *114*:492–497. https://doi.org/10.1073/pnas.1613855114

Braet, F., Spector, I., De Zanger, R., & Wisse, E. (1998). A novel structure involved in the formation of liver endothelial cell fenestrae revealed by using the actin inhibitor misakinolide. *Proceedings of the National Academy of Sciences of the United States of America*, *95*:13635–13640. https://doi.org/10.1073/pnas.95.23.13635

Breslin, J. W., Zhang, X. E., Worthylake, R. A., & Souza-Smith, F. M. (2015). Involvement of local lamellipodia in endothelial barrier function. *PLoS ONE*, *10*:e0117970. https://doi.org/10.1371/journal.pone.0117970

Bubb, M. R., Senderowicz, A. M. J., Sausville, E. A., Duncan, K. L. K., & Korn, E. D. (1994). Jasplakinolide, a cytotoxic natural product, induces actin polymerization and competitively inhibits the binding of phalloidin to F-actin. *Journal of Biological Chemistry*, *269*:14869–14871. Retrieved from https://www.jbc.org/content/269/21/14869

Bubb, M. R., Spector, I., Beyer, B. B., & Fosen, K. M. (2000). Effects of jasplakinolide on the kinetics of actin polymerization. An explanation for certain in vivo observations. *Journal of Biological Chemistry*, *275*:5163–5170. https://doi.org/10.1074/jbc.275.7.5163

Carey, S. P., Charest, J. M., & Reinhart-King, C. A. (2010). Forces during cell adhesion and spreading: Implications for cellular homeostasis. In A. Gefen (Ed.), *Cellular and Biomolecular Mechanics and Mechanobiology. Studies in Mechanobiology, Tissue Engineering and Biomaterials* (Vol. 4, pp. 29–69). Springer. https://doi.org/10.1007/8415_2010_22

Carmeliet, P. (2003). Angiogenesis in health and disease. *Nature Medicine*, *9*(6), 653–660. https://doi.org/10.1038/nm0603-653

Cavo, M., Fato, M., Peñuela, L., Beltrame, F., Raiteri, R., & Scaglione, S. (2016). Microenvironment complexity and matrix stiffness regulate breast cancer cell activity in a 3D in vitro model. *Scientific Reports*, *6*:35367. https://doi.org/10.1038/srep35367

Ceccarelli, J., Cheng, A., & Putnam, A. J. (2012). Mechanical strain controls endothelial patterning during angiogenic sprouting. *Cellular and Molecular Bioengineering*, *5*:463–473. https://doi.org/10.1007/s12195-012-0242-y

Charras, G., & Sahai, E. (2014). Physical influences of the extracellular environment on cell migration. *Nature Reviews Molecular Cell Biology*, *15*:813–824. https://doi.org/10.1038/nrm3897

Chartier, L., Rankin, L. L., Allen, R. E., Kato, Y., Fusetani, N., Karaki, H., … Hartshorne, D. J. (1991). Calyculin - A increases the level of protein phosphorylation and changes the shape of 3T3 fibroblasts. *Cytoskeleton*, *18*:26–40. https://doi.org/10.1002/cm.970180104

Chervin-Pétinot, A., Courçon, M., Almagro, S., Nicolas, A., Grichine, A., Grunwald, D., … Gulino-Debrac, D. (2012). Epithelial protein lost in neoplasm (EPLIN) interacts with α-catenin and actin filaments in endothelial cells and stabilizes vascular capillary network in vitro. *The Journal of Biological Chemistry*, *287*:7556–7572. https://doi.org/10.1074/jbc.M111.328682

Cóndor, M., Steinwachs, J., Mark, C., García-Aznar, J. M., & Fabry, B. (2017). Traction force microscopy in 3-dimensional extracellular matrix networks. *Current Protocols in Cell Biology*, *75*:10.22.1-10.22.20. https://doi.org/10.1002/cpcb.24

Conte, I. L., Hellen, N., Bierings, R., Mashanov, G. I., Manneville, J.-B., Kiskin, N. I., … Carter, T. (2016). Interaction between MyRIP and the actin cytoskeleton regulates Weibel – Palade body trafficking and exocytosis. *Journal of Cell Science*, *129*:592–603. https://doi.org/10.1242/jcs.178285

Cooper, J. A. (1987). Effects of cytochalasin and phalloidin on actin. *The Journal of Cell Biology*, *105*:1473–1478. https://doi.org/10.1083/jcb.105.4.1473

Crews, P., Manes, L. V, & Boehler, M. (1986). Jasplakinolide, a cyclodepsipeptide from the marine sponge, Jaspis SP. *Tetrahedron Letters*, *27*:2797–2800. https://doi.org/10.1016/S0040-4039(00)84645-6

De Smet, F., Segura, I., De Bock, K., Hohensinner, P. J., Carmeliet, P., Bock, K. De, & Hohensinner, P. J. (2009). Mechanisms of vessel branching: filopodia on endothelial tip cells lead the way. *Arteriosclerosis, Thrombosis, and Vascular Biology*, *29*:639–649. https://doi.org/10.1161/ATVBAHA.109.185165

Doyle, A. D., Carvajal, N., Jin, A., Matsumoto, K., & Yamada, K. M. (2015). Local 3D matrix microenvironment regulates cell migration through spatiotemporal dynamics of contractility-dependent adhesions. *Nature Communications*, *6*:8720. https://doi.org/10.1038/ncomms9720

Doyle, A. D., Petrie, R. J., Kutys, M. L., & Yamada, K. M. (2013). Dimensions in cell migration. *Current Opinion in Cell Biology*, *25*:642–649. https://doi.org/10.1016/j.ceb.2013.06.004

Doyle, A. D., Wang, F. W., Matsumoto, K., & Yamada, K. M. (2009). One-dimensional topography underlies three-dimensional fibrillar cell migration. *The Journal of Cell Biology*, *184*:481–490. https://doi.org/10.1083/jcb.200810041

Du, Y., Herath, S. C. B., Wang, Q.-G., Wang, D.-A., Asada, H. H., & Chen, P. C. Y. (2016). Three-dimensional characterization of mechanical interactions between endothelial cells and extracellular matrix during angiogenic sprouting. *Scientific Reports*, *6*:21362. https://doi.org/10.1038/srep21362

Du, Y., Herath, S. C. B., Wang, Q. G., Asada, H., & Chen, P. C. Y. (2018). Determination of Green's function for three-dimensional traction force reconstruction based on geometry and boundary conditions of cell culture matrices. *Acta Biomaterialia*, *67*:215–228. https://doi.org/10.1016/j.actbio.2017.12.002

Edgar, L. T., Hoying, J. B., Utzinger, U., Underwood, C. J., Krishnan, L., Baggett, B. K., … Weiss, J. a. (2014). Mechanical interaction of angiogenic microvessels with the extracellular matrix. *Journal of Biomechanical Engineering*, *136*:021001_1-021001_15. https://doi.org/10.1115/1.4026471

Edgar, L. T., Underwood, C. J., Guilkey, J. E., Hoying, J. B., & Weiss, J. a. (2014). Extracellular matrix density regulates the rate of neovessel growth and branching in sprouting angiogenesis. *PLoS ONE*, *9*:e85178. https://doi.org/10.1371/journal.pone.0085178

Elliott, H., Fischer, R. S., Myers, K. A., Desai, R. A., Gao, L., Chen, C. S., … Danuser, G. (2015). Myosin II controls cellular branching morphogenesis and migration in three dimensions by minimizing cell-surface curvature. *Nature Cell Biology*, *17*:137–147. https://doi.org/10.1038/ncb3092

Fabian, L., Troscianczuk, J., & Forer, A. (2007). Calyculin A, an enhancer of myosin, speeds up anaphase chromosome movement. *Cell and Chromosome*, *6*:42–45. https://doi.org/10.1186/1475-9268-6-1

Farooqui, R., & Fenteany, G. (2005). Multiple rows of cells behind an epithelial wound edge extend cryptic lamellipodia to collectively drive cell-sheet movement. *Journal of Cell Science*, *118*:51–63. https://doi.org/10.1242/jcs.01577

Fischer, R. S., Gardel, M., Ma, X., Adelstein, R. S., & Waterman, C. M. (2009). Local cortical tension by myosin II guides 3D endothelial cell branching. *Current Biology*, *19*:260–265. https://doi.org/10.1016/j.cub.2008.12.045

Fletcher, D. A., & Mullins, R. D. (2010). Cell mechanics and the cytoskeleton. *Nature*, *463*:485–492. https://doi.org/10.1038/nature08908

Folkman, J. (2007). Angiogenesis: an organizing principle for drug discovery? *Nature Reviews Drug Discovery*, *6*:273–286. https://doi.org/10.1038/nrd2115

Fraley, S. I., Feng, Y., Krishnamurthy, R., Kim, D.-H., Celedon, A., Longmore, G. D., & Wirtz, D. (2010). A distinctive role for focal adhesion proteins in three-dimensional cell motility. *Nature Cell Biology*, *12*:598–604. https://doi.org/10.1038/ncb2062

Friedl, P., & Gilmour, D. (2009). Collective cell migration in morphogenesis, regeneration and cancer. *Nature Reviews Molecular Cell Biology*, *10*:445–457. https://doi.org/10.1038/nrm2720

Gerhardt, H. (2008). VEGF and endothelial guidance in angiogenic sprouting. *Organogenesis*, *4*: 241–246. https://doi.org/10.4161/org.4.4.7414

Geudens, I., & Gerhardt, H. (2011). Coordinating cell behaviour during blood vessel formation. *Development*, *138*:4569–4583. https://doi.org/10.1242/dev.062323

Ghibaudo, M., Di Meglio, J. M., Hersen, P., & Ladoux, B. (2011). Mechanics of cell spreading within 3D-micropatterned environments. *Lab on a Chip*, *11*:805–812. https://doi.org/10.1039/c0lc00221f

Gjorevski, N., Piotrowski, A. S., Varner, V. D., & Nelson, C. M. (2015). Dynamic tensile forces drive collective cell migration through three-dimensional extracellular matrices. *Scientific Reports*, *5*:11458. https://doi.org/10.1038/srep11458

Glazier, R., Brockman, J. M., Bartle, E., Mattheyses, A. L., Destaing, O., & Salaita, K. (2019). DNA mechanotechnology reveals that integrin receptors apply pN forces in podosomes on fluid substrates. *Nature Communications*, *10*:1–13. https://doi.org/10.1038/s41467-019-12304-4

Goeckeler, Z. M., Bridgman, P. C., & Wysolmerski, R. B. (2008). Nonmuscle myosin II is responsible for maintaining endothelial cell basal tone and stress fiber integrity. *American Journal of Physiology: Cell Physiology*, *295*:994–1006. https://doi.org/10.1152/ajpcell.00318.2008

Gupton, S. L., & Waterman-Storer, C. M. (2006). Spatiotemporal feedback between actomyosin and focal-adhesion systems optimizes rapid cell migration. *Cell*, *125*:1361–1374. https://doi.org/10.1016/j.cell.2006.05.029

Haeger, A., Wolf, K., Zegers, M. M., & Friedl, P. (2015). Collective cell migration: guidance principles and hierarchies. *Trends in Cell Biology*, *25*:556–566. https://doi.org/10.1016/j.tcb.2015.06.003

Hall, M. S., Long, R., Feng, X., Huang, Y. L., Hui, C. Y., & Wu, M. (2013). Toward single cell traction microscopy within 3D collagen matrices. *Experimental Cell Research*, *319*:2396–2408. https://doi.org/10.1016/j.yexcr.2013.06.009

Hetheridge, C., Scott, A. N., Swain, R. K., Copeland, J. W., Higgs, H. N., Bicknell, R., & Mellor, H. (2012). The formin FMNL3 is a cytoskeletal regulator of angiogenesis. *Journal of Cell Science*, *125*:1420–1428. https://doi.org/10.1242/jcs.091066

Hohmann, & Dehghani. (2019). The cytoskeleton - A complex interacting meshwork. *Cells*, *8*:362. https://doi.org/10.3390/cells8040362

Holy, M., & Brautigan, D. L. (2012). Calyculin a from Discodermia calyx is a dual action toxin that blocks calcium influx and inhibits protein Ser/Thr phosphatases. *Toxins*, *4*:940–954. https://doi.org/10.3390/toxins4100940

Holzinger, A. (2001). Jasplakinolide. An actin-specific reagent that promotes actin polymerization. In R. H. Gavin (Ed.), *Cytoskeleton Methods and Protocols. Methods in Molecular Biology* (Vol. 161, pp. 109–120). Humana Press. https://doi.org/10.1385/1-59259-051-9:109

Hui, K. L., Balagopalan, L., Samelson, L. E., & Upadhyaya, A. (2015). Cytoskeletal forces during signaling activation in Jurkat T-cells. *Molecular Biology of the Cell*, *26*:685–695. https://doi.org/10.1091/mbc.E14-03-0830

Hung, W.-C., Chen, S.-H., Paul, C. D., Stroka, K. M., Lo, Y.-C., Yang, J. T., & Konstantopoulos, K. (2013). Distinct signaling mechanisms regulate migration in unconfined versus confined spaces. *The Journal of Cell Biology*, *202*:807–824. https://doi.org/10.1083/jcb.201302132

Huveneers, S., Oldenburg, J., Spanjaard, E., van der Krogt, G., Grigoriev, I., Akhmanova, A., … de Rooij, J. (2012). Vinculin associates with endothelial VE-cadherin junctions to control force-dependent remodeling. *The Journal of Cell Biology*, *196*:641–652. https://doi.org/10.1083/jcb.201108120

Hyland, C., Mertz, A. F., Forscher, P., & Dufresne, E. (2014). Dynamic peripheral traction forces balance stable neurite tension in regenerating

Aplysia bag cell neurons. *Scientific Reports*, *4*:1–8. https://doi.org/10.1038/srep04961
Iacobazzia, D., Garaeva, I., Albertario, A., Cherif, M., Angelini, G. D., Caputo, M., & Ghorbel, M. T. (2015). Protein phosphatase 1 beta is modulated by chronic hypoxia and involved in the angiogenic endothelial cell migration. *Cell Physiology and Biochemistry*, *36*:384–394. https://doi.org/10.1159/000430257
Indra, I., Undyala, V., Kandow, C., Thirumurthi, U., Dembo, M., & Beningo, K. A. (2011). An in vitro correlation of mechanical forces and metastatic capacity. *Physical Biology*, *8*:1–23. https://doi.org/10.1088/1478-3975/8/1/015015
Ingber, D. E. (2002). Mechanical signaling and the cellular response to extracellular matrix in angiogenesis and cardiovascular physiology. *Circulation Research*, *91*:877–887. https://doi.org/10.1161/01.RES.0000039537.73816.E5

Ingber, D. E. (2008). Tensegrity-based mechanosensing from macro to micro. *Progress in Biophysics and Molecular Biology*, *97*:163–179. https://doi.org/10.1016/j.pbiomolbio.2008.02.005

Ishihara, H., Martin, B. L., Brautigan, D. L., Karaki, H., Ozaki, H., Kato, Y., … Hartshorne, D. J. (1989). Calyculin A and okadaic acid: Inhibitors of protein phosphatase activity. *Biochemical and Biophysical Research Communications*, *159*:871–877. https://doi.org/10.1016/0006-291X(89)92189-X

Ishihara, H., Ozaki, H., Sato, K., Hori, M., Karaki, H., Watabe, S., … Hartshorne, D. J. (1989). Calcium-independent activation of contractile apparatus in smooth muscle by calyculin-A. *Journal of Pharmacology and Experimental Therapeutics*, *250*:388–396. Retrieved from http://jpet.aspetjournals.org/content/250/1/388

Izquierdo-Álvarez, A., Vargas, D. A., Jorge-Peñas, Á., Subramani, R., Vaeyens, M. M., & Van Oosterwyck, H. (2019). Spatiotemporal analyses of cellular tractions describe subcellular effect of substrate stiffness and coating. *Annals of Biomedical Engineering*, *47*:624–637. https://doi.org/10.1007/s10439-018-02164-2

Jerrell, R. J., & Parekh, A. (2014). Cellular traction stresses mediate extracellular matrix degradation by invadopodia. *Acta Biomaterialia*, *10*:1886–1896. https://doi.org/10.1016/j.actbio.2013.12.058

Jiang, J., Zhang, Z. hong, Yuan, X. bin, & Poo, M. ming. (2015). Spatiotemporal dynamics of traction forces show three contraction centers in migratory neurons. *Journal of Cell Biology*, *209*:759–774. https://doi.org/10.1083/jcb.201410068

Jing, X., Sun, J., Zhang, X., Tang, K., Yin, Q., Wu, H., … Cheng, M. (2013). Jasplakinolide affects the functions of HUVECs via actin stabilization. *Chinese Pharmacological Bulletin*, *29*:1079–1083. https://doi.org/10.3969/j.issn.1001-1978.2013.08.010

Jorge-Peñas, A., Bové, H., Sanen, K., Vaeyens, M.-M., Steuwe, C., Roeffaers, M., … Van Oosterwyck, H. (2017). 3D full-field quantification of cell-induced large deformations in fibrillar biomaterials by combining non-rigid image registration with label-free second harmonic generation. *Biomaterials*, *136*:86–97. https://doi.org/10.1016/j.biomaterials.2017.05.015

Jorge-Peñas, A., Izquierdo-Alvarez, A., Aguilar-Cuenca, R., Vicente-Manzanares, M., Garcia-Aznar, J. M., Van Oosterwyck, H., … Muñoz-Barrutia, A. (2015). Free form deformation–based image registration improves accuracy of traction force microscopy. *PLoS ONE*, *10*:e0144184:1-22. https://doi.org/10.1371/journal.pone.0144184

Ju, R., Cirone, P., Lin, S., Griesbach, H., Slusarski, D. C., & Crews, C. M. (2010). Activation of the planar cell polarity formin DAAM1 leads to inhibition of endothelial cell proliferation, migration, and angiogenesis. *Proceedings of the National Academy of Sciences of the United States of America*, *107*:6906–6911. https://doi.org/10.1073/pnas.1001075107

Katoh, K., Kano, Y., & Ookawara, S. (2008). Role of stress fibers and focal adhesions as a mediator for mechano-signal transduction in endothelial cells in situ. *Vascular Health and Risk Management*, *4*:1273–1282. https://doi.org/10.2147/vhrm.s3933

Kim, J., Jones, C. A. R., Groves, N. S., & Sun, B. (2016). Three-dimensional reflectance traction microscopy. *PLoS ONE*, *11*:e0156797. https://doi.org/10.1371/journal.pone.0156797

Kniazeva, E., & Putnam, A. J. (2009). Endothelial cell traction and ECM density influence both capillary morphogenesis and maintenance in 3-D. *American Journal of Physiology: Cell Physiology*, *297*:C179–C187. https://doi.org/10.1152/ajpcell.00018.2009

Kniazeva, E., Weidling, J. W., Singh, R., Botvinick, E. L., Digman, M. A., Gratton, E., & Putnam, A. J. (2012). Quantification of local matrix deformations and mechanical properties during capillary morphogenesis in 3D. *Integrative Biology*, *4*:431–439. https://doi.org/10.1039/c2ib00120a

Koch, T. M., Münster, S., Bonakdar, N., Butler, J. P., & Fabry, B. (2012). 3D traction forces in cancer cell invasion. *PLoS ONE*, *7*:e33467. https://doi.org/10.1371/journal.pone.0033476

Koestler, S. A., Auinger, S., Vinzenz, M., Rottner, K., & Small, J. V. (2008). Differentially oriented populations of actin filaments generated in lamellipodia collaborate in pushing and pausing at the cell front. *Nature Cell Biology*, *10*:306–313. https://doi.org/10.1038/ncb1692

Köhn, M. (2017). Miklós Bodanszky Award Lecture: Advances in the selective targeting of protein phosphatase-1 and phosphatase-2A with peptides. *Journal of Peptide Science*, *23*:749–756. https://doi.org/10.1002/psc.3033

Kolega, J. (2006). The role of myosin II motor activity in distributing myosin asymmetrically and coupling protrusive activity to cell translocation. *Molecular Biology of the Cell*, *17*:4435–4445. https://doi.org/10.1091/mbc.E06-05-0431

Kovács, M., Tóth, J., Hetényi, C., Málnási-Csizmadia, A., & Seller, J. R. (2004). Mechanism of blebbistatin inhibition of myosin II. *Journal of Biological Chemistry*, *279*:35557–35563. https://doi.org/10.1074/jbc.M405319200

Kraning-Rush, C. M., Califano, J. P., & Reinhart-King, C. A. (2012). Cellular traction stresses increase with increasing metastatic potential. *PLoS ONE*, *7*:e32572. https://doi.org/10.1371/journal.pone.0032572

Kraning-Rush, C. M., Carey, S. P., Califano, J. P., Smith, B. N., & Reinhart-King, C. A. (2011). The role of the cytoskeleton in cellular force generation in 2D and 3D environments. *Physical Biology*, *8*:015009. https://doi.org/10.1088/1478-3975/8/1/015009

Kubow, K. E., Conrad, S. K., & Horwitz, A. R. (2013). Matrix microarchitecture and myosin II determine adhesion in 3D matrices. *Current Biology*, *23*:1607–1619. https://doi.org/10.1016/j.cub.2013.06.053

Kumar, A., Maitra, A., Sumit, M., Ramaswamy, S., & Shivashankar, G. V. (2014). Actomyosin contractility rotates the cell nucleus. *Scientific Reports*, *4*:3781. https://doi.org/10.1038/srep03781

Leckband, D., & Israelachvili, J. (2001). Intermolecular forces in biology. In *Quarterly Reviews of Biophysics*, *34*:105-267. https://doi.org/10.1017/s0033583501003687

Lee, P.-F., Bai, Y., Smith, R. L., Bayless, K. J., & Yeh, A. T. (2013). Angiogenic responses are enhanced in mechanically and microscopically characterized, microbial transglutaminase crosslinked collagen matrices with increased stiffness. *Acta Biomaterialia*, *9*:7178–7190. https://doi.org/10.1016/j.actbio.2013.04.001

Lee, S., Zeiger, A., Maloney, J. M., Kotecki, M., Van Vliet, K. J., & Herman, I. M. (2010). Pericyte actomyosin-mediated contraction at the cell – material interface can modulate the microvascular niche. *Journal of Physics: Condensed Matter*, *22*:194115. https://doi.org/10.1088/0953-8984/22/19/194115

Lemmon, C. A., Chen, C. S., & Romer, L. H. (2009). Cell traction forces direct fibronectin matrix assembly. *Biophysical Journal*, *96*:729–738. https://doi.org/10.1016/j.bpj.2008.10.009

Limouze, J., Straight, A. F., Mitchison, T., & Sellers, J. R. (2004). Specificity of blebbistatin, an inhibitor of myosin II. *Journal of Muscle Research and Cell Motility*, *25*:337–341. https://doi.org/10.1007/s10974-004-6060-7

Liu, Z., Tan, J. L., Cohen, D. M., Yang, M. T., Sniadecki, N. J., Ruiz, S. A., … Chen, C. S. (2010). Mechanical tugging force regulates the size of cell-cell junctions. *Proceedings of the National Academy of Sciences of the United States of America*, *107*:9944–9949. https://doi.org/10.1073/pnas.0914547107

Lu, L., Oswald, S. J., Ngu, H., & Yin, F. C. P. (2008). Mechanical properties of actin stress fibers in living cells. *Biophysical Journal*, *95*:6060–6071. https://doi.org/10.1529/biophysj.108.133462

Mabeta, P., & Pepper, M. S. (2009). A comparative study on the anti-angiogenic effects of DNA-damaging and cytoskeletal-disrupting agents. *Angiogenesis*, *12*:81–90. https://doi.org/10.1007/s10456-009-9134-8

Malandrino, A., Trepat, X., Kamm, R. D., & Mak, M. (2019). Dynamic filopodial forces induce accumulation, damage, and plastic remodeling of 3D extracellular matrices. *PLoS Computational Biology*, *15*:e1006684. https://doi.org/10.1371/journal.pcbi.1006684

Mammoto, T., Mammoto, A., & Ingber, D. E. (2013). Mechanobiology and developmental control. *Annual Review of Cell and Developmental Biology*, *29*:27–61. https://doi.org/10.1146/annurev-cellbio-101512-122340

Martins, G. G., & Kolega, J. (2006). Endothelial cell protrusion and migration in three-dimensional collagen matrices. *Cell Motility and the Cytoskeleton*, *63*:101–115. https://doi.org/10.1002/cm.20104

Mason, B. N., Starchenko, A., Williams, R. M., Bonassar, L. J., & Reinhart-King, C. A. (2013). Tuning three-dimensional collagen matrix stiffness independently of collagen concentration modulates endothelial cell behavior. *Acta Biomaterialia*, *9*:4635–4644. https://doi.org/10.1016/j.actbio.2012.08.007

Mierke, C. T. (2013). The integrin alphav beta3 increases cellular stiffness and cytoskeletal remodeling dynamics to facilitate cancer cell invasion. *New Journal of Physics*, *15*:015003 (23pp). https://doi.org/10.1088/1367-2630/15/1/015003

Miron-Mendoza, M., Seemann, J., & Grinnell, F. (2010). The differential regulation of cell motile activity through matrix stiffness and porosity in three dimensional collagen matrices. *Biomaterials*, *31*:6425–6435. https://doi.org/10.1016/j.biomaterials.2010.04.064

Moreno-Arotzena, O., Borau, C., Movilla, N., Vicente-Manzanares, M., & Garcia-Aznar, J. M. (2015). Fibroblast migration in 3D is controlled by haptotaxis in a non-muscle myosin II-dependent manner. *Annals of Biomedical Engineering*, *43*:3025–3039. https://doi.org/10.1007/s10439-015-1343-2

Mseka, T., & Cramer, L. P. (2011). Actin depolymerization-based force retracts the cell rear in polarizing and migrating cells. *Current Biology*, *21*:2085–2091. https://doi.org/10.1016/j.cub.2011.11.006

Munevar, S., Wang, Y., & Dembo, M. (2001). Traction force microscopy of migrating normal and H-ras transformed 3T3 fibroblasts. *Biophysical Journal*, *80*:1744–1757. https://doi.org/10.1016/S0006-3495(01)76145-0

Myers, K. A., Applegate, K. T., Danuser, G., Fischer, R. S., & Waterman, C. M. (2011). Distinct ECM mechanosensing pathways regulate microtubule dynamics to control endothelial cell branching morphogenesis. *The Journal of Cell Biology*, *192*:321–334. https://doi.org/10.1083/jcb.201006009

Nandakumar, V., English, A. E., Moy, A. B., Mahfouz, M., Ward, R., Kruse, K., … Goldman, M. H. (2004). Real time monitoring of endothelial cell actin filament disruption by cytochalasin D using a cellular impedance biosensor. *2nd IEEE/EMBS International Summer School on Medical Devices and Biosensors*, 85–86. https://doi.org/10.1109/ISSMD.2004.1689567

Ng, M. R., Besser, A., Danuser, G., & Brugge, J. S. (2012). Substrate stiffness regulates cadherin-dependent collective migration through myosin-II contractility. *The Journal of Cell Biology*, *199*:545–563. https://doi.org/10.1083/jcb.201207148

Oakes, P. W., Banerjee, S., Marchetti, M. C., & Gardel, M. L. (2014). Geometry regulates traction stresses in adherent cells. *Biophysical Journal*, *107*:825–833. https://doi.org/10.1016/j.bpj.2014.06.045

Pedersen, J. A., & Swartz, M. A. (2005). Mechanobiology in the tird dimension. *Annals of Biomedical Engineering*, *33*:1469–1490. https://doi.org/10.1007/s10439-005-8159-4

Peschetola, V., Laurent, V. M., Duperray, A., Michel, R., Ambrosi, D., Preziosi, L., & Verdier, C. (2013). Time-dependent traction force microscopy for cancer cells as a measure of invasiveness. *Cytoskeleton*, *70*:201–214. https://doi.org/10.1002/cm.21100

Peterson, J. R., & Mitchison, T. J. (2002). Small molecules, big impact: A history of chemical inhibitors and the cytoskeleton. *Chemistry & Biology*, *9*:1275–1285. https://doi.org/10.1016/S1074-5521(02)00284-3

Petrie, R. J., Koo, H., & Yamada, K. M. (2014). Generation of compartmentalized pressure by a nuclear piston governs cell motility in a 3D matrix. *Science*, *345*:1062–1065. https://doi.org/10.1126/science.1256965

Pospich, S., Merino, F., & Raunser, S. (2020). Structural effects and functional implications of phalloidin and jasplakinolide binding to actin filaments. *Structure*, *28*:437-449.e5. https://doi.org/10.1016/j.str.2020.01.014

Provenzano, P. P., & Keely, P. J. (2011). Mechanical signaling through the cytoskeleton regulates cell proliferation by coordinated focal adhesion and Rho GTPase signaling. *Journal of Cell Science*, *124*:1195–1205. https://doi.org/10.1242/jcs.067009

Santos-Oliveira, P., Correia, A., Rodrigues, T., Ribeiro-Rodrigues, T. M., Matafome, P., Rodríguez-Manzaneque, J. C., … Travasso, R. D. M. (2015). The force at the tip - modelling tension and proliferation in sprouting angiogenesis. *PLoS Computational Biology*, *11*:e1004436. https://doi.org/10.1371/journal.pcbi.1004436

Sasse, F., Kunze, B., Gronewold, T. M. A., & Reichenbach, H. (1998). The chondramides: Cytostatic agents from myxobacteria acting on the actin cytoskeleton. *Journal of the National Cancer Institute*, *90*:1559–1563. https://doi.org/10.1093/jnci/90.20.1559

Sauteur, L., Krudewig, A., Herwig, L., Ehrenfeuchter, N., Lenard, A., Affolter, M., & Belting, H.-G. (2014). Cdh5/VE-cadherin promotes endothelial cell interface elongation via cortical actin polymerization during angiogenic sprouting. *Cell Reports*, *9*:504–513. https://doi.org/10.1016/j.celrep.2014.09.024

Sawyer, S. J., Norvell, S. M., Ponik, S. M., & Pavalko, F. M. (2001). Regulation of PGE 2 and PGI 2 release from human umbilical vein endothelial cells by actin cytoskeleton. *American Journal of Physiology: Cell Physiology*, *281*:C1038–C1045. https://doi.org/10.1152/ajpcell.2001.281.3.C1038

Scherlach, K., Boettger, D., Remme, N., & Hertweck, C. (2010). The chemistry and biology of cytochalasans. *Natural Product Reports*, *27*:869–886. https://doi.org/10.1039/b903913a

Schliwa, M. (1982). Action of cytochalasin D on cytoskeletal networks. *The Journal of Cell Biology*, *92*:79–91. https://doi.org/10.1083/jcb.92.1.79

Schmidt, M., Paes, K., De Mazière, A., Smyczek, T., Yang, S., Gray, A., … Ye, W. (2007). EGFL7 regulates the collective migration of endothelial cells by restricting their spatial distribution. *Development*, *134*:2913–2923. https://doi.org/10.1242/dev.002576

Shamloo, A., & Heilshorn, S. C. (2010). Matrix density mediates polarization and lumen formation of endothelial sprouts in VEGF gradients. *Lab on a Chip*, *10*:3061–3068. https://doi.org/10.1039/c005069e

Shoji, K., Ohashi, K., Sampei, K., Oikawa, M., & Mizuno, K. (2012). Cytochalasin D acts as an inhibitor of the actin-cofilin interaction. *Biochemical and Biophysical Research Communications*, *424*:52–57. https://doi.org/10.1016/j.bbrc.2012.06.063

Silberberg, Y. R., Mieda, S., Amemiya, Y., Sato, T., Kihara, T., Nakamura, N., … Nakamura, C. (2013). Evaluation of the actin cytoskeleton state using an antibody-functionalized nanoneedle and an AFM. *Biosensors and Bioelectronic*, *40*:3–9. https://doi.org/10.1016/j.bios.2012.06.044

Sim, J. Y., Moeller, J., Hart, K. C., Ramallo, D., Vogel, V., Dunn, A. R., … Pruitt, B. L. (2015). Spatial distribution of cell-cell and cell-ECM adhesions regulates force balance while maintaining E-cadherin molecular tension in cell pairs. *Molecular Biology of the Cell*, *26*:2456–2465. https://doi.org/10.1091/mbc.E14-12-1618

Steinwachs, J., Metzner, C., Skodzek, K., Lang, N., Thievessen, I., Mark, C., … Fabry, B. (2016). Three-dimensional force microscopy of cells in biopolymer networks. *Nature Methods*, *13*:171–176. https://doi.org/10.1038/nmeth.3685

Straight, A. F., Cheung, A., Limouze, J., Chen, I., Westwood, N. J., Sellers, J. R., & Mitchison, T. J. (2003). Dissecting temporal and spatial control of cytokinesis with a myosin II inhibitor. *Science*, *299*:1743–1747. https://doi.org/10.1126/science.1081412

Stricker, J., Aratyn-Schaus, Y., Oakes, P. W., & Gardel, M. L. (2011). Spatiotemporal constraints on the force-dependent growth of focal adhesions. *Biophysical Journal*, *100*:2883–2893. https://doi.org/10.1016/j.bpj.2011.05.023

Su, S.-C., Mendoza, E. A., Kwak, H.-I., & Bayless, K. J. (2008). Molecular profile of endothelial invasion of three-dimensional collagen matrices: insights into angiogenic sprout induction in wound healing. *American Journal of Physiology: Cell Physiology*, *295*:C1215–C1229. https://doi.org/10.1152/ajpcell.00336.2008

Sung, K. E., Su, G., Pehlke, C., Trier, S. M., Eliceiri, K. W., Keely, P. J., … Beebe, D. J. (2010). Control of 3-dimensional collagen matrix polymerization for reproducible Human Mammary Fibroblast cell culture in microfluidic devices. *Biomaterials*, *30*:4833–4841. https://doi.org/10.1016/j.biomaterials.2009.05.043

Swingle, M., Ni, L., & Honkanen, R. E. (2007). Small molecule inhibitors of Ser/Thr protein phosphatases: Specificity, use and common forms of abuse. In G. Moorhead (Ed.), *Protein Phosphatase Protocols. Methods in Molecular Biology* (Vol. 365, pp. 23–38). Springer. https://doi.org/10.1385/1-59745-267-X:23

Tee, S.-Y., Fu, J., Chen, C. S., & Janmey, P. A. (2011). Cell shape and substrate rigidity both regulate cell stiffness. *Biophysical Journal*, *100*:L25–L27. https://doi.org/10.1016/j.bpj.2010.12.3744

Thievessen, I., Fakhri, N., Steinwachs, J., Kraus, V., McIsaac, R. S., Gao, L., … Fabry, B. (2015). Vinculin is required for cell polarization, migration, and extracellular matrix remodeling in 3D collagen. *The FASEB Journal*, *29*:4555–4567. https://doi.org/10.1096/fj.14-268235

Travasso, R. D. M. (2011). The mechanics of blood vessel growth. In D. T. Simionescu & A. Simionescu (Eds.), *Vasculogenesis and Angiogenesis - from Embryonic Development to Regenerative Medicine* (pp. 187–204). IntechOpen. https://doi.org/10.5772/34615

Tse, J. R., & Engler, A. J. (2010). Preparation of hydrogel substrates with tunable mechanical properties. *Current Protocols in Cell Biology*, *47*, 10.16.1-10.16.16. https://doi.org/10.1002/0471143030.cb1016s47

Vaeyens, M. M., Jorge-Peñas, A., Barrasa-Fano, J., Steuwe, C., Heck, T., Carmeliet, P., … Van Oosterwyck, H. (2020). Matrix deformations around angiogenic sprouts correlate to sprout dynamics and suggest pulling activity. *Angiogenesis*. https://doi.org/10.1007/s10456-020-09708-y

Versaevel, M., Grevesse, T., & Gabriele, S. (2012). Spatial coordination between cell and nuclear shape within micropatterned endothelial cells. *Nature Communications*, *3*:671. https://doi.org/10.1038/ncomms1668

Vickerman, V., Blundo, J., Chung, S., & Kamm, R. D. (2008). Design, fabrication and implementation of a novel multi parameter control microfluidic platform for three-dimensional cell culture and real-time imaging. *Lab on a Chip*, *8*:1468–1477. https://doi.org/10.1039/b802395f

Vickerman, V., Kim, C., & Kamm, R. D. (2013). Microfluidic devices for angiogenesis. In C. A. Reinhart-King (Ed.), *Mechanical and Chemical Signaling in Angiogenesis. Studies in Mechanobiology, Tissue Engineering and Biomaterials* (pp. 93–120). Springer. https://doi.org/10.1007/978-3-642-30856-7_5

Visegrády, B., Lorinczy, D., Hild, G., Somogyi, B., & Nyitrai, M. (2004). The effect of phalloidin and jasplakinolide on the flexibility and thermal stability of actin filaments. *FEBS Letters*, *565*:163–166. https://doi.org/10.1016/j.febslet.2004.03.096

Wakatsuki, T., Schwab, B., Thompson, N. C., & Elson, E. L. (2001). Effects of cytochalasin D and latrunculin B on mechanical properties of cells. *Journal of Cell Science*, *114*:1025–1036. Retrieved from https://jcs.biologists.org/content/114/5/1025

Wang, N., Tytell, J. D., & Ingber, D. E. (2009). Mechanotransduction at a distance: Mechanically coupling the extracellular matrix with the nucleus. *Nature Reviews Molecular Cell Biology*, *10*:75–82. https://doi.org/10.1038/nrm2594

Wang, Shuaijun, Crevenna, A. H., Ugur, I., Marion, A., Antes, I., Kazmaier, U., … Zahler, S. (2019). Actin stabilizing compounds show specific biological effects due to their binding mode. *Scientific Reports*, *9*:9731. https://doi.org/10.1038/s41598-019-46282-w

Wang, Shue, Sun, J., Xiao, Y., Lu, Y., Zhang, D. D., & Wong, P. K. (2017). Intercellular tension negatively regulates angiogenic sprouting of endothelial tip cells via Notch1-Dll4 signaling. *Advanced Biosystems*, *1*:1600019. https://doi.org/10.1002/adbi.201600019

Waschke, J., Curry, F. E., Adamson, R. H., & Drenckhahn, D. (2004). Regulation of actin dynamics is critical for endothelial barrier functions. *American Journal of Physiology: Heart and Circulatory Physiology*, *288*:H1296–H1305. https://doi.org/10.1152/ajpheart.00687.2004

Winer, J. P., Oake, S., & Janmey, P. A. (2009). Non-linear elasticity of extracellular matrices enables contractile cells to communicate local position and orientation. *PLoS ONE*, *4*:e6382. https://doi.org/10.1371/journal.pone.0006382

Wolfenson, H., Meacci, G., Liu, S., Stachowiak, M. R., Iskratsch, T., Ghassemi, S., … Sheetz, M. P. (2016). Tropomyosin controls sarcomere-like contractions for rigidity sensing and suppressing growth on soft matrices. *Nature Cell Biology*, *18*:33–42. https://doi.org/10.1038/ncb3277

Yoon, C., Choi, C., Stapleton, S., Mirabella, T., Howes, C., Dong, L., … Chen, C. S. (2019). Myosin IIA–mediated forces regulate multicellular integrity during vascular sprouting. *Molecular Biology of the Cell*, *30*:1974–1984. https://doi.org/10.1091/mbc.e19-02-0076

Zeng, G., Taylor, S. M., McColm, J. R., Kappas, N. C., Kearney, J. B., Williams, L. H., … Bautch, V. L. (2007). Orientation of endothelial cell division is regulated by VEGF signaling during blood vessel formation. *Blood*, *109*:1345–1352. https://doi.org/10.1182/blood-2006-07-037952

FIGURE 1 Targeting the acto-myosin network of endothelial cells with small molecules. (a) *The F-actin cytoskeleton of endothelial cells treated for 24 hours with DMSO (Ctr), blebbistatin (Blebb), calyculinA (CalA), cytochalasin D (CytoD) or jasplakinolide (Jasp). Cells were transduced with adenoviral LifeAct-RFP for visualizing the F-actin (actin, grey).* ***(b)*** *Sketch illustrating the antagonistic modes of action of the compounds. NMMII = Non-Muscle Myosin II. MLCP = Myosin Light Chain Phosphatase.*

FIGURE 2 Growing and visualizing endothelial invasion and sprouting into collagen. (a) *Sketch of the model design (see also Methods and Supplementary Figure S2).* ***(b)*** *Timelapse of endothelial sprouts growing in collagen (HUVEC cells transduced with LifeAct-GFP2 for live F-actin visualization).* ***(c-d)*** *Multicellular sprouts grown over 24 hours, fixed, stained (Alexa488-Phalloidin, grey, actin; DAPI, blue, nucleus) and imaged with confocal fluorescence microscopy, with increasing level of detail.* ***(e)*** *Stimulated emission depletion (STED) microscopy of a sprout tip.*

FIGURE 3 Semi-automated quantification and characterization of the invasive response. (a) *Representative image of filtered microscopy data from an invasive response.* ***(b)*** *Distance quantification from collagen boundary to sprout tips.* ***(c)*** *Detection of detached cells and quantification of detached cell area and distance (defined by the distance at which 90 % of the detached cell area is covered).* ***(d)*** *Quantification of the total segmented sprout area (total area minus detached area).* ***(e-f)*** *Segmentation of the nuclei before (e) and after (f) filtering the nuclei within the sprout area. All panels are based on the same field of view in (a).*

FIGURE 4 Effect of blebbistatin on in vitro sprouting and HUVEC cytoskeleton. (a) *Representative confocal images of endothelial invasion, sprouts and 2D migrating HUVEC cells grown within an imaging chamber and treated with DMSO (Ctr) or blebbistatin (Blebb) for 24 hours. HUVEC cells and sprouts were stained with Alexa488-Phalloidin (grey, actin) and DAPI (bleu, nucleus).* ***(b)*** *Sketch of the mode of action of blebbistatin.* ***(c-e)*** *Quantification of the invasion experiments showing projected area (c), invasion distance (d) and number of nuclei (e) of sprouts grown in DMSO or blebbistatin. # nuclei = number of nuclei; ** for $p < 0.01$, *** for $p < 0.001$.*

FIGURE 5 Effect of calyculin A on HUVEC cytoskeleton, endothelial invasion and sprout morphology. (a) *Representative confocal images of endothelial invasion, sprouts and 2D migrating HUVEC cells grown within an imaging chamber and treated with DMSO (Ctr) or calyculin A (CalA) for 24 hours. HUVEC cells and sprouts were stained with Alexa488-Phalloidin (grey, actin) and DAPI (bleu, nucleus).* ***(b)*** *Sketch of the mode of action of calyculin A. MLCK ROCK = myosin light chain kinase ROCK.* ***(c-e)*** *Quantification of the invasion experiments showing projected area (c), invasion distance (d) and number of nuclei (e) of sprouts grown in DMSO or calyculin A. # nuclei = number of nuclei; ** for $p < 0.01$.*

FIGURE 6 Effect of cytochalasin D and jasplakinolide on endothelial invasion, sprout morphology, HUVEC cytoskeleton and cellular tractions. (a) *Sketch of the mode of action of cytochalasin D (CytoD) and jasplakinolide (Jasp).* ***(b)*** *Confocal images of endothelial invasion, sprouts and 2D migrating HUVEC cells grown within an imaging chamber and treated with cytochalasin D or jasplakinolide for 24 hours. HUVEC cells and sprouts were stained with Alexa488-Phalloidin (grey, actin) and DAPI (blue, nucleus).* ***(c-e)*** *Quantification of the invasion experiments showing projected area (c), invasion distance (d) and number of nuclei (e) of sprouts grown in DMSO (Ctr), cytochalasin D or jasplakinolide.* ***(f)*** *Total traction force magnitudes of single HUVEC cells spread on collagen-coated polyacrylamide gels before (left datapoints) and after (right datapoints) 1h of treatment with DMSO (Ctr), CytoD or Jasp. See*

*Supplementary Figure S4 and Supplementary Table 4 for statistics of the Traction Force Microscopy experiments. # nuclei = number of nuclei; * for $p < 0.05$; *** for $p < 0.001$.*

(a)

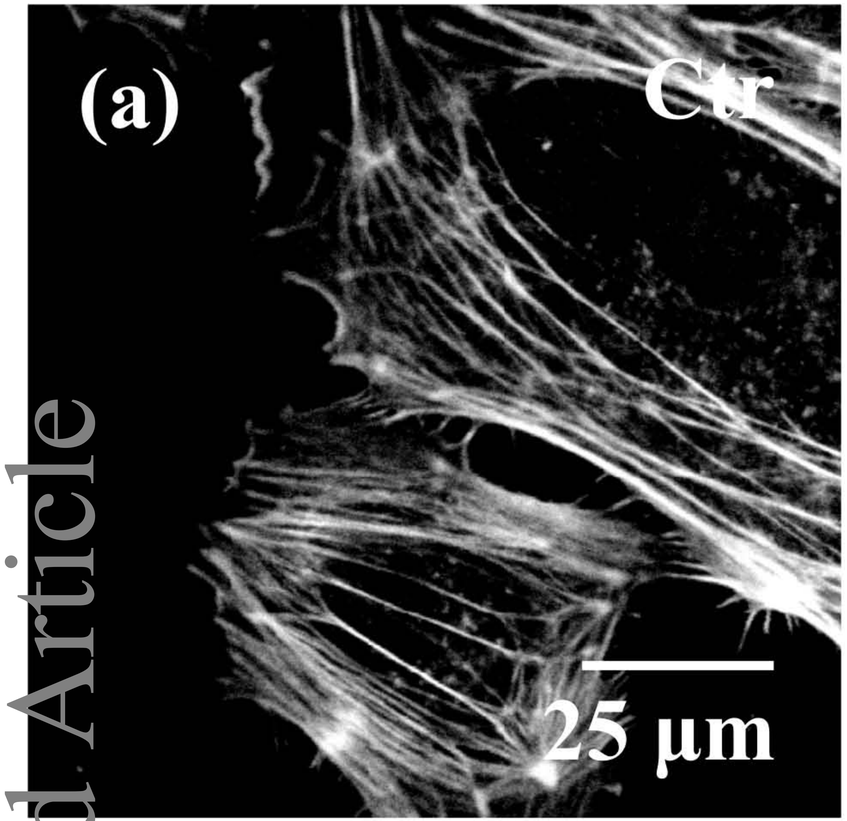

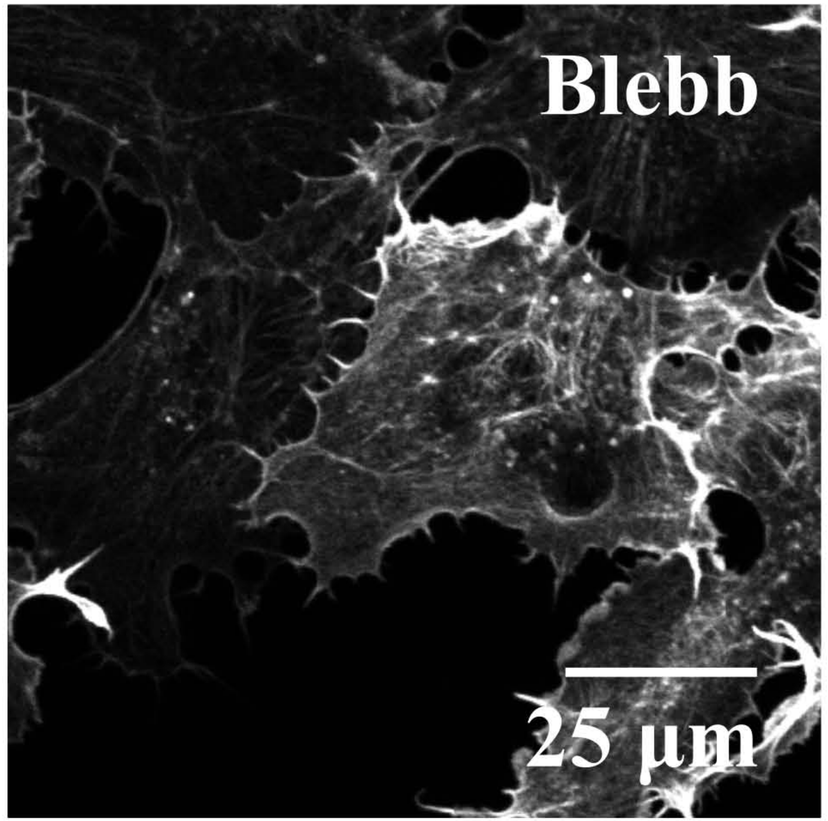

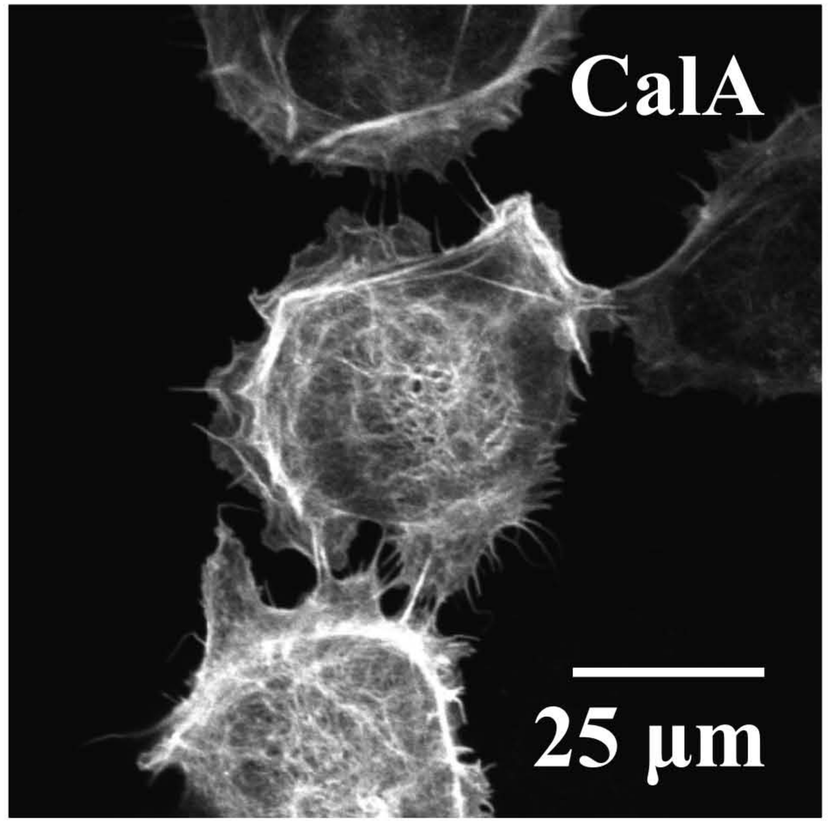

(b)

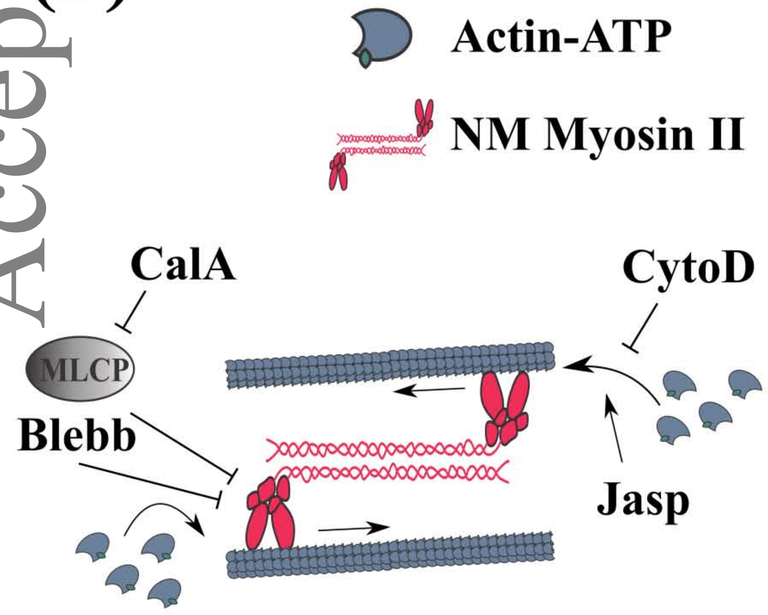

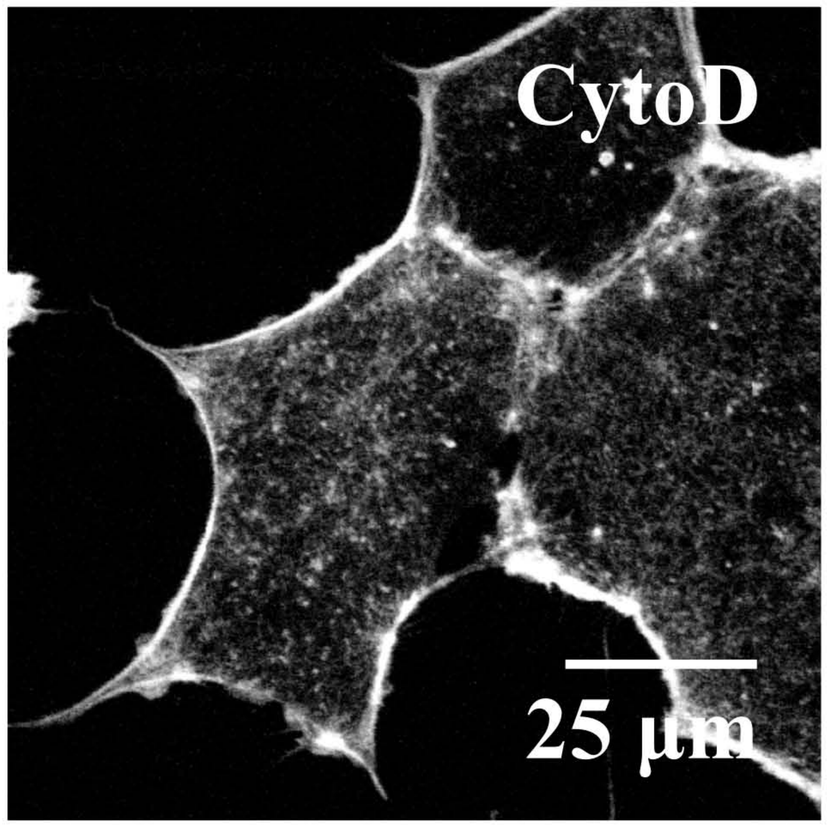

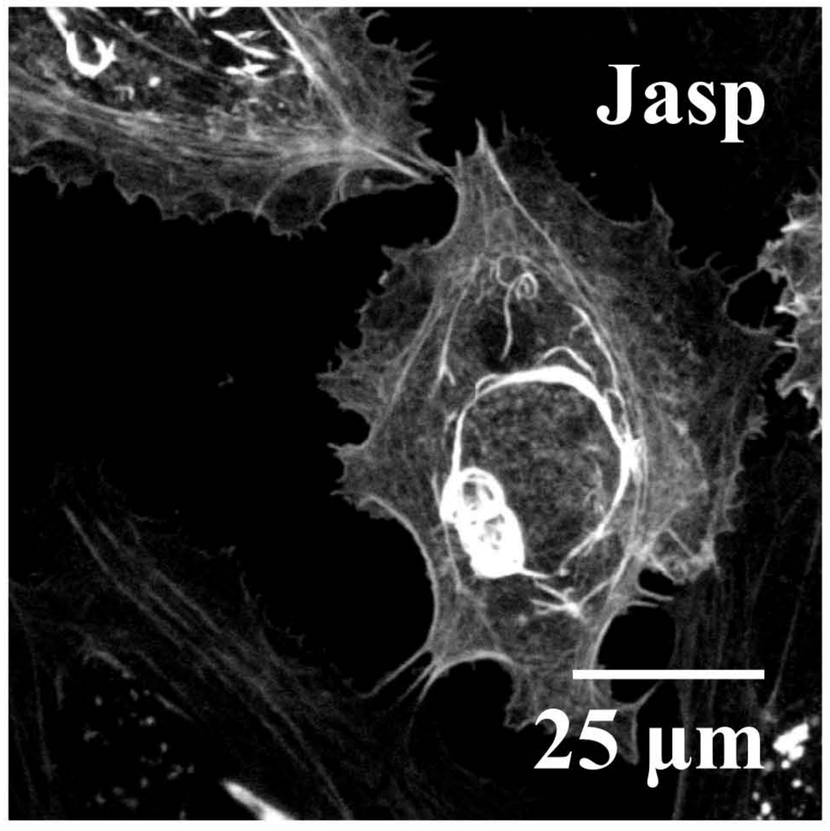

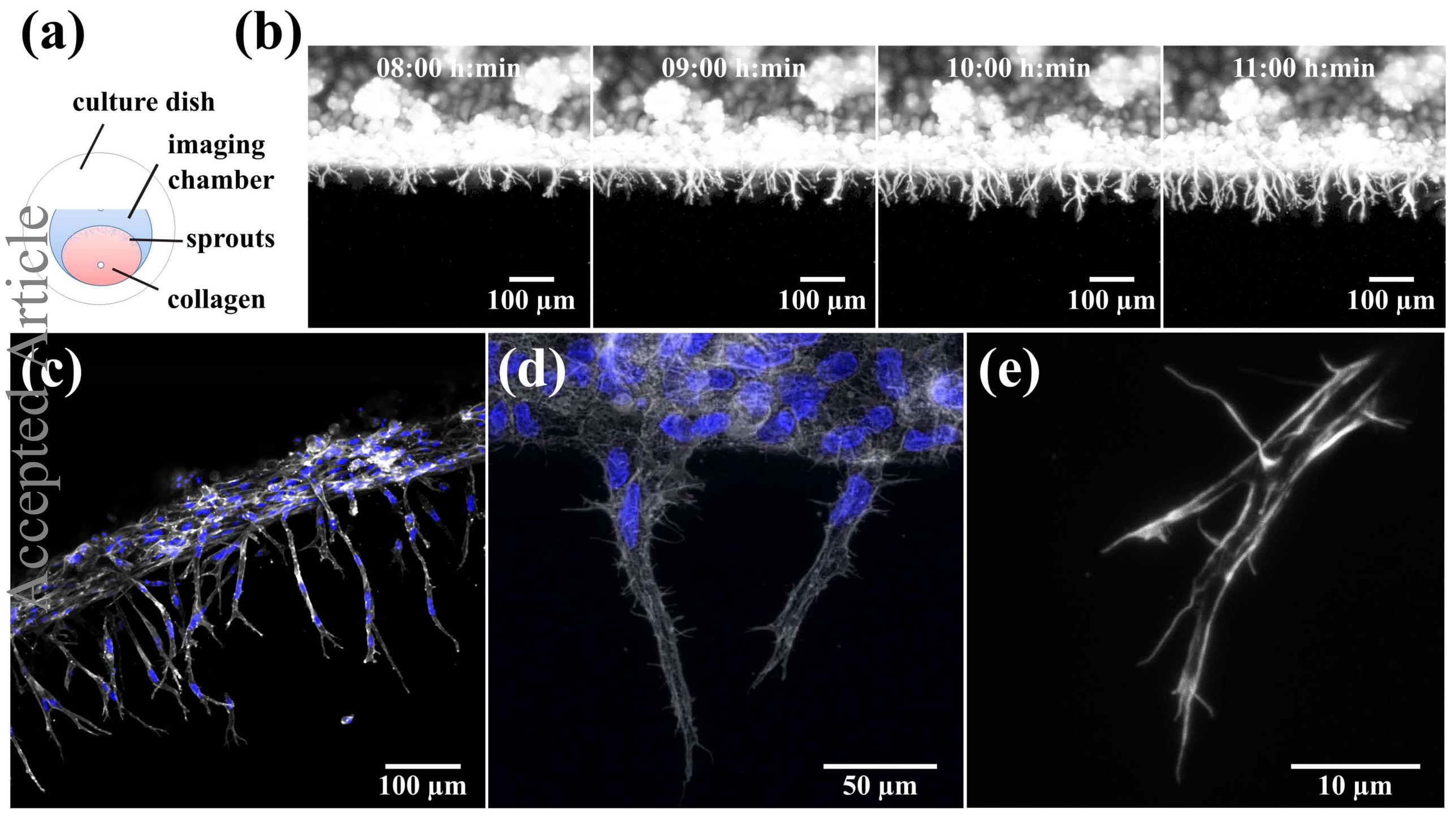

(a)

200 µm

Filtered microscopy data

(b) 0 395 µm

Invasion distance

(c)

Detached cell area

Detached cell distance

(d)

Segmented sprouts

Sprout area

(e)

Segmented nuclei

(f)

Sprout nuclei

(a)

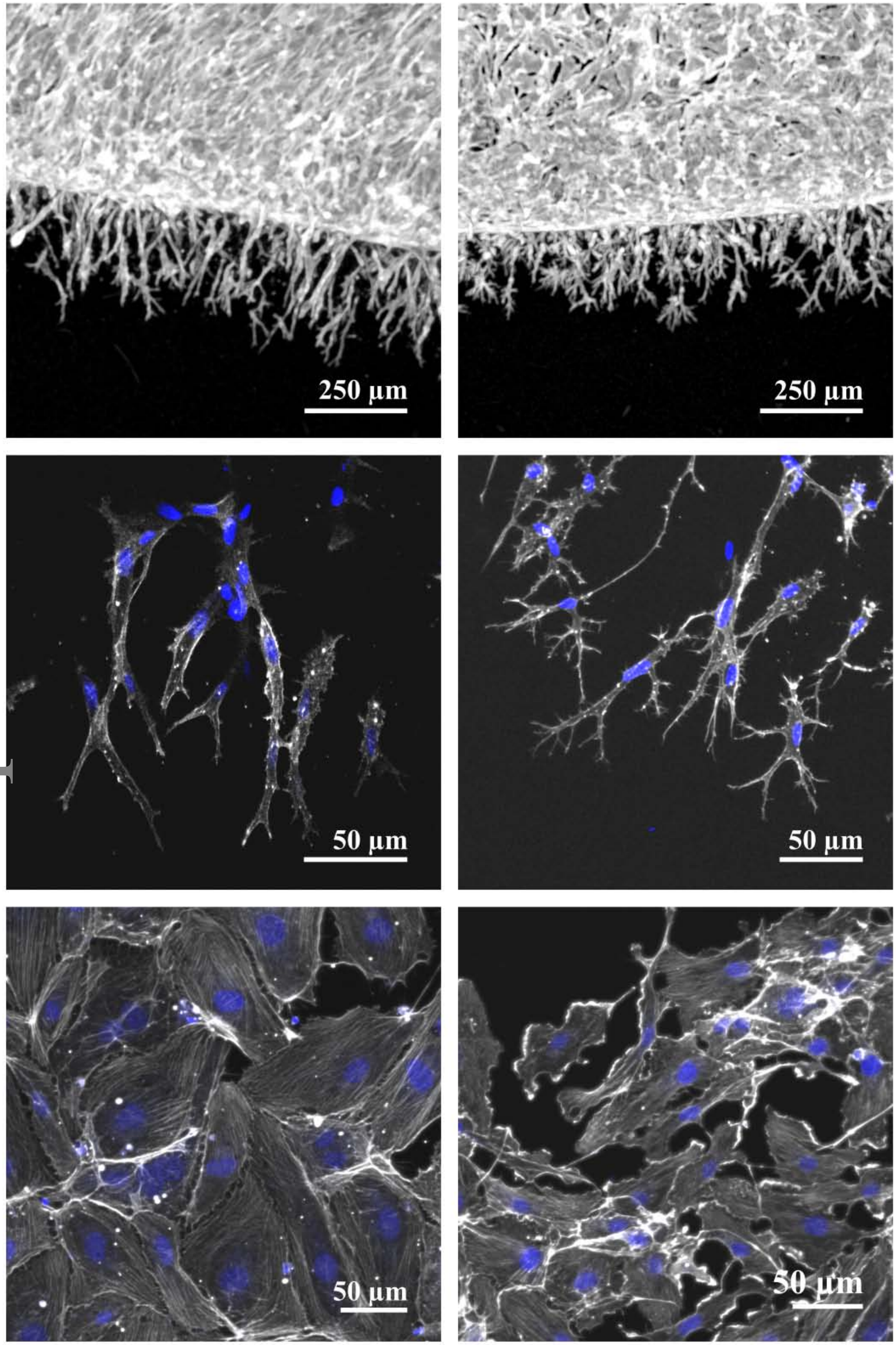

(b)

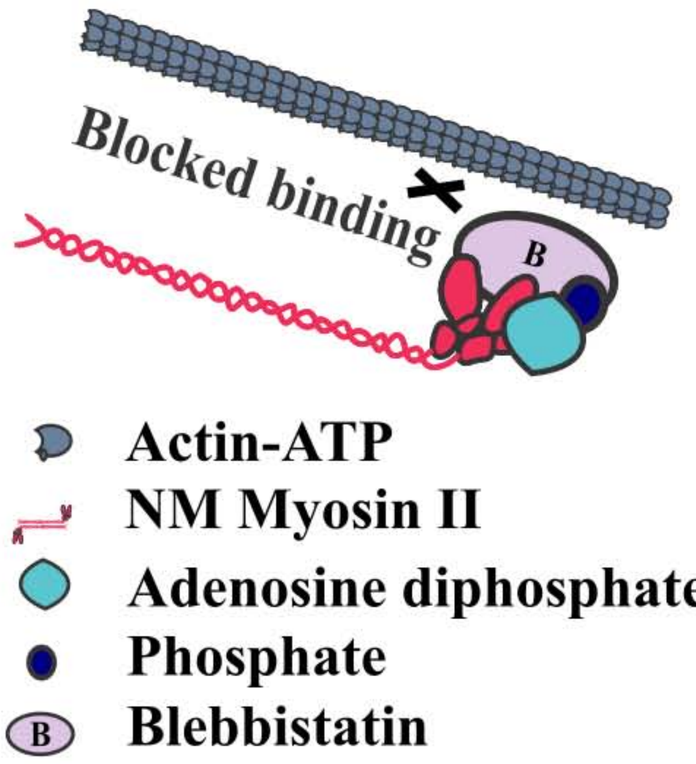

(c)

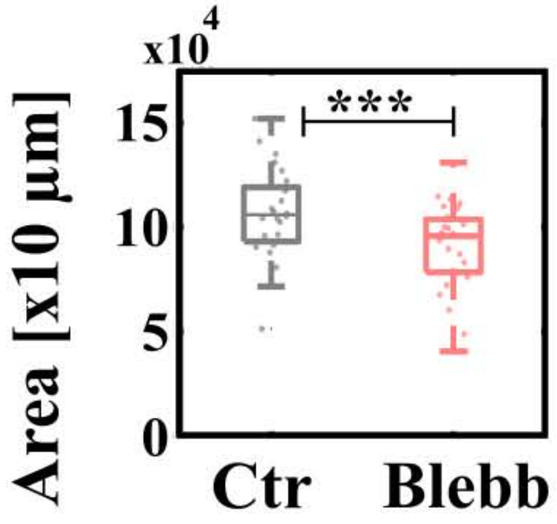

(d)

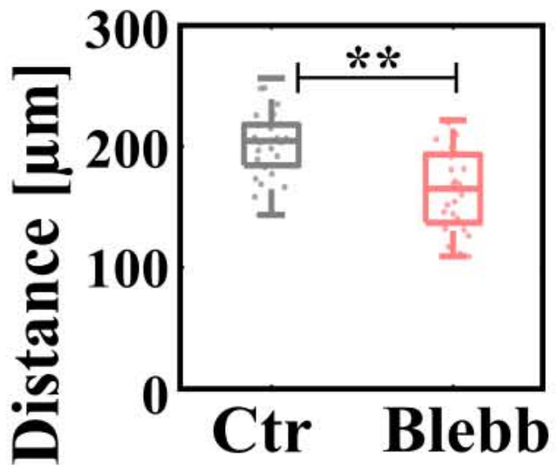

(e)

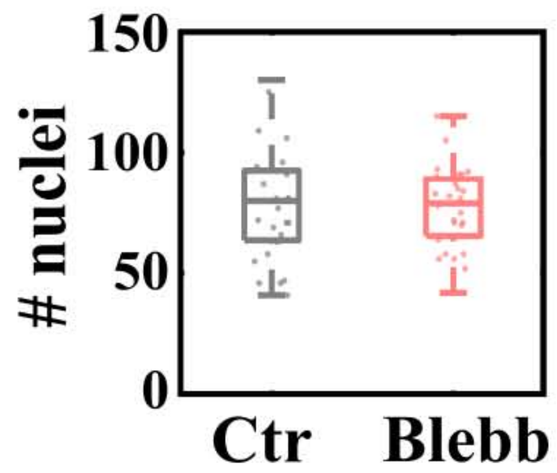

(a)

Ctr

CalA

2D cells

Invasion

250 µm

250 µm

50 µm

50 µm

50 µm

50 µm

(b)

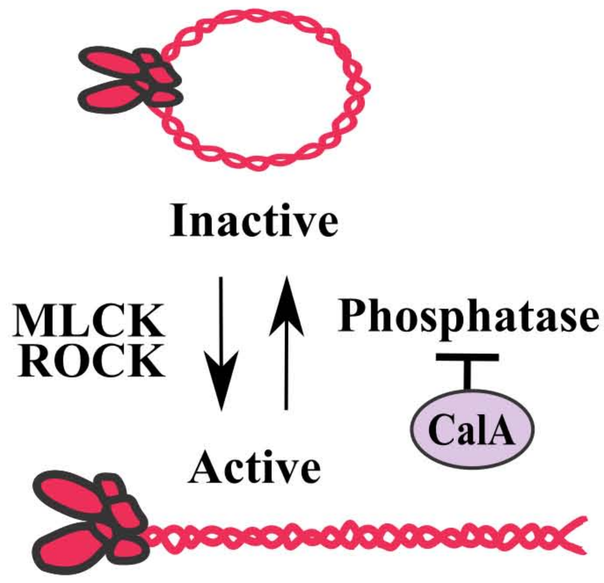

(c)

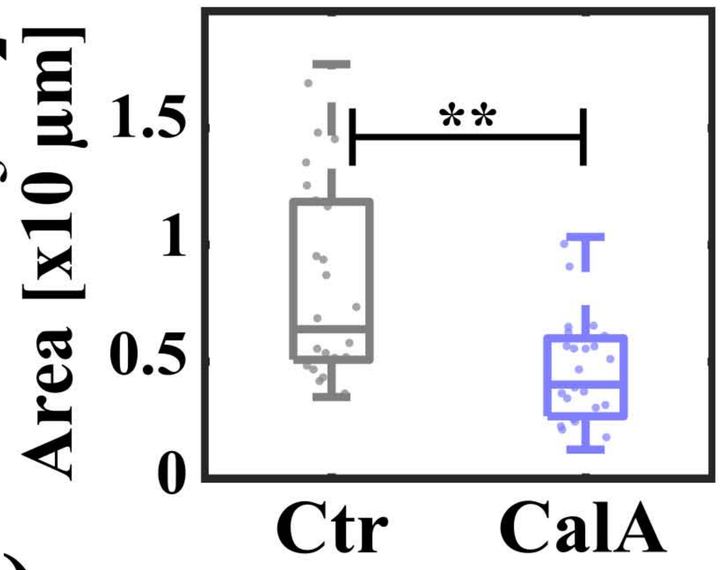

(d)

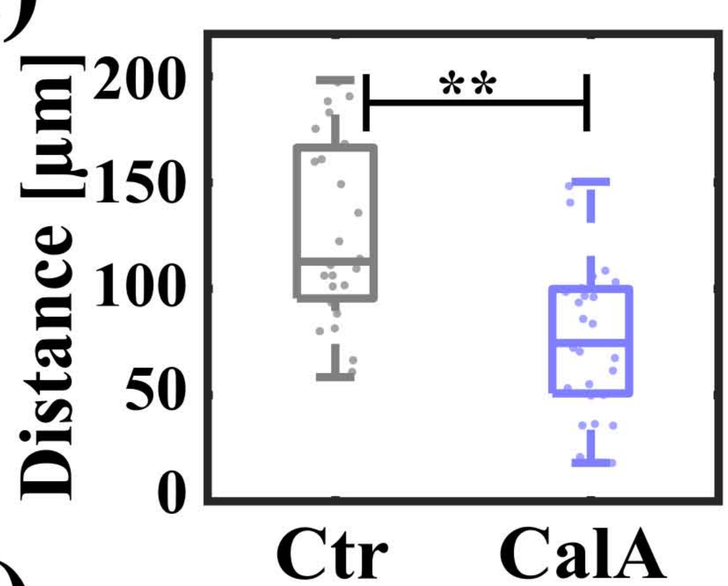

(e)

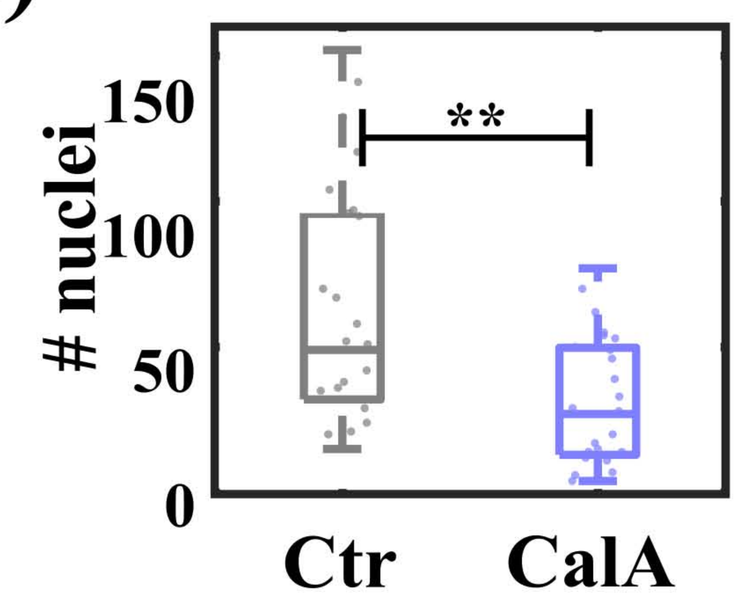

(a)

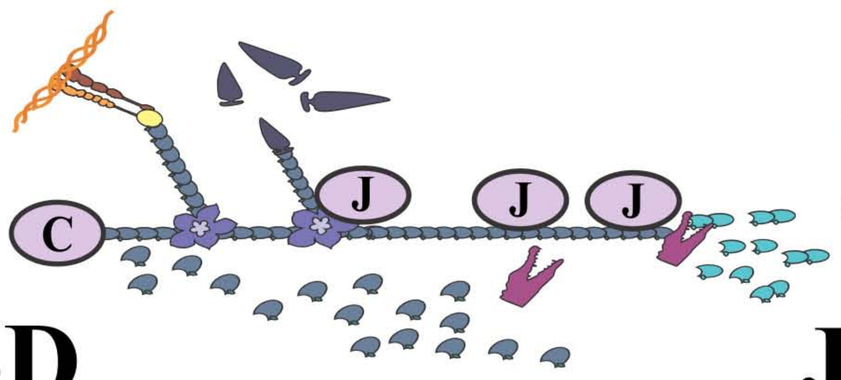

C Cytochalasin D
J Jasplakinolide
Actin-ATP
Actin-ADP
Capping protein
Cofilin

CytoD Jasp

(b)

2D cells

250 µm
250 µm
50 µm
50 µm
50 µm
50 µm

(c)

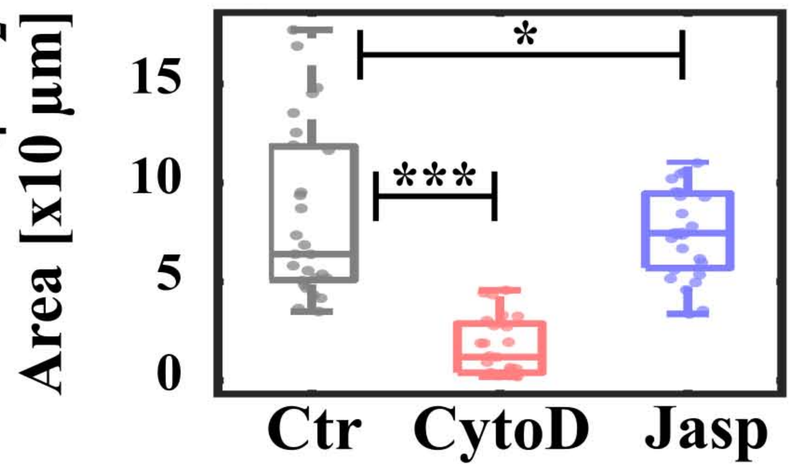

(d)

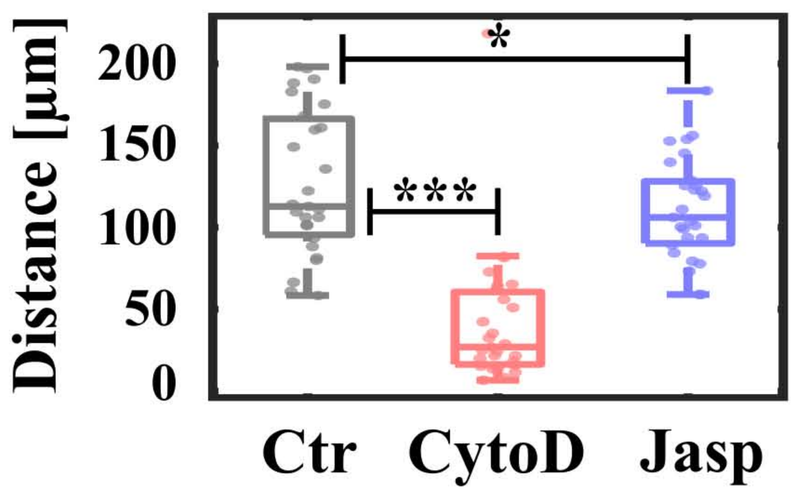

(e)

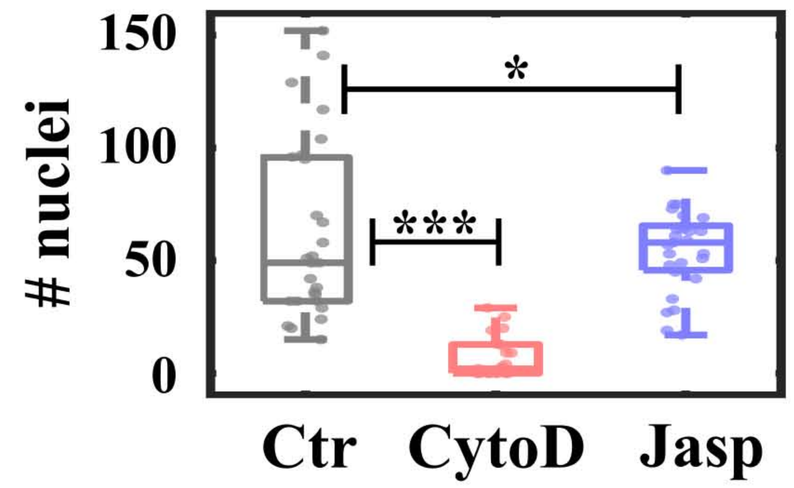

(f)